The $\Delta I = 1/2$ Rule and the Strong Coupling Expansion

Thesis by

Ian Gareth Angus

In Partial Fulfillment of the Requirements

for the Degree of

Doctor of Philosophy

California Institute of Technology

Pasadena, California

1986

(Submitted May 20, 1986)

Acknowledgments

I would like to thank John Preskill for his guidance and help while I have been at Caltech.

I would like to acknowledge the hospitality of the staff and students of Cornell University's Laboratory of Nuclear Studies, and at the Fermi National Accelerator Laboratory, where parts of this work were done.

I would also like to thank Claude Bernard, Marco Bochicchio, Sumit Das, Soo-Jong Rey, and Mark Wise, for many very helpful discussions. I also acknowledge the aid of Courtenay Footman and Marc Goroff for answering many questions about computers.

Partial financial support for this work was provided by the New Zealand Postgraduate Scholarship, and the Feynman Fellowship.

The computer calculations were done on the UNIX VAX 11/780 "Cithep" and part of the software was developed on the UNIX VAX 11/750 "Lnsvax" at Cornell University's Laboratory of Nuclear Studies.

Finally, I dedicate this thesis to my parents, Paul and Beverly Angus; and to Robin, in recognition of, above all, their patience.

ABSTRACT

We will attempt to understand the *Delta I Equals One Half* pattern of the nonleptonic weak decays of the Kaons. The calculation scheme employed is the Strong Coupling Expansion of lattice QCD. Kogut-Susskind fermions are used in the Hamiltonian formalism. We will describe in detail the methods used to expedite this calculation, almost all of which was done by computer algebra.

The final result is very encouraging. Even though an exact interpretation is clouded by the presence of irrelevant operators, a distinct signal of the *Delta I Equals One Half* Rule is observed. With an appropriate choice of the one free parameter, enhancements as great as those observed experimentally can be obtained along with a qualitative prediction for the relative magnitudes of the CP violating phases.

We also point out a number of surprising results which we turn up in the course of the calculation. The computer methods employed are briefly described.

Table of Contents

Figure Captions

1. (1a) Feynman diagrams : K^+ decay.

   (1b) Feynman diagrams : K^0 decays.

2. Kogut–Susskind Fermion Sublattices

3. Strong Coupling and Computer Algebra.

4. Components of the Two Pion Wave Function:

   (4a) Separated

   (4b) Side by side

   (4c) Head to tail

   (4d) Head to head

5. (5a) Zeroth–Order Graph

   (5b) First–Order Graphs

6. (6a) "Penguin" or "Eye" Graphs; u Loop

   (6b) "Penguin" or "Eye" Graphs; c Loop

7. Matrix Elements $\langle 0 | H_W | K \rangle$ and $\langle 2 | H_W | K \rangle$

8. The Ratio ε'/ε

1 : Introduction

In the time since it was introduced, Quantum Chromodynamics, or QCD, has become widely accepted as the best available theory of the strong interactions. This has happened despite the paucity of good quantitative support for the theory, although there is a significant qualitative agreement between theory and experiment.

In this thesis we present a calculation of the weak matrix elements relevant to the empirical $\Delta I = 1/2$ rule observed to hold for the nonleptonic weak decays of Kaons. The calculation will be carried out in the Strong Coupling limit and to second order in perturbation theory beyond this limit. This calculation is meant to be a *first* attempt at a first principles calculation. As a result, a number of severe assumptions will be made in the hope that as we gain experience we will be able to relax these assumptions. We should not expect too much from such a calculation; agreement to within a factor of two will be considered to be satisfactory.

First, we will review the K data and the theoretical techniques of strong coupling. Then we will describe, in overview, how the Strong Coupling expansion could be, and has in part been, implemented as a specialized symbolic manipulation system. Then we plunge headfirst into setting up, and finally, executing the desired calculation. Finally, we will make a few remarks about the results.

The calculations will be performed using Kogut–Susskind fermions in the Hamiltonian formalism. Using this method has many virtues, but also some annoying detractions. These will be described as we come to them.

2 : The Kaon Data

Of the multitude of hadrons that have been observed in nature to date, the Kaons $K^{\pm}$, $K^0\,\overline{K}^0$ (or $K_s\,K_L$) have provided us with arguably the most interesting systems in which to study the physics of both the strong and weak interactions. These particles contain a single s, or $\overline{s}$, quark; the lightest quark that we do not normally encounter in nature, and yet we can produce them in copious amounts so enabling detailed and accurate experimental study. Of course, the most spectacular feature of the $K^0\,\overline{K}^0$ system is that it is the only example in nature for which we have been able to observe CP violation. However, the motivation for turning our attention to the Kaons is not CP violation but another prominent feature of the weak interactions of Kaons, the empirical $\Delta I = 1/2$ rule. In the following two tables we present some experimental data about the Kaons[1]. To keep these results in perspective, we have also presented the decays adjacent in rate to those we will be concerned with.

K^+

Mass : 493.667±0.015 MeV

Lifetime : $(1.2371 \pm 0.0026) \times 10^{-8}$ s

Decay Products	Branching Ratio	p_π , MeV/c
$\mu^+\nu_\mu$	0.6351 ± 0.0016	236
$\pi^+\pi^0$	0.2117 ± 0.0015	205
$\pi^+\pi^+\pi^-$	0.0559 ± 0.0003	125

K^0 (K_S)

Mass : 497.67 ± 0.13 MeV

Lifetime : (0.8923 ± 0.0022) × 10^{-10} s

Decay Products	Branching Ratio	p_π , MeV/c
$\pi^+\pi^-$	0.6861± 0.0024	206
$\pi^0\pi^0$	0.3139±0.0024	209
$\pi^+\pi^-\gamma$	$(1.85\pm0.10)\times10^{-5}$	206

The decays we wish to focus upon are the nonleptonic decays into two pions. There is just enough phase space to allow three pion decays but these are strongly suppressed by the kinematics relative to the two pion decay modes and we shall therefore not consider them further. Because the Kaons are 0^- particles they decay in the S–wave channel; hence, the decay rate can be immediately calculated to be:

$$\Gamma_a = \frac{p_\pi}{8\pi m_K} |f_a|^2 \tag{2.1}$$

where p_π is the momentum of the outgoing pions and f_a is the invariant amplitude for the channel a. The combination of decay rates that we are interested in is:

$$\frac{\Gamma(K^+ \to \pi^+\pi^0)}{\Gamma(K^0 \to \pi^+\pi^-) + \Gamma(K^0 \to \pi^0\pi^0)} \approx \frac{1}{655} \tag{2.2}$$

This is an amazing experimental result, for if we simply guessed this ratio we probably would have suggested a value of order unity.

Let us probe a little more deeply. The pion has isospin $I = 1$; hence, the possible final state wave functions of the two pions are the isospin states:

$$I = 2 \; I_3 = 1 \; : \quad \frac{1}{\sqrt{2}}(\pi^+ \pi^0 + \pi^0 \pi^+) \tag{2.3a}$$

$$I = 2 \; I_3 = 0 \; : \quad \frac{1}{\sqrt{6}}(\pi^+ \pi^- + 2\pi^0 \pi^0 + \pi^- \pi^+) \tag{2.3b}$$

$$I = 0 \; I_3 = 0 \; : \quad \frac{1}{\sqrt{3}}(\pi^+ \pi^- - \pi^0 \pi^0 + \pi^- \pi^+) \tag{2.3c}$$

Because the Kaons have $I = 1/2$ we immediately see that the K^+ decay is pure $\Delta I = 3/2$ whereas the K^0 decay channels derive from an admixture of $\Delta I = 1/2$ and $\Delta I = 3/2$ amplitudes. With (2.3), the definitions:

$$f_{3/2} \, e^{i\delta_{3/2}} = \left\langle I=2, I_3=0 \; \left| H_{3/2}^{(\Delta s = 1)} \right| \; I=1/2, I_3=1/2 \right\rangle \tag{2.4a}$$

$$f_{1/2} \, e^{i\delta_{1/2}} = \left\langle I=0, I_3=0 \; \left| H_{1/2}^{(\Delta s = 1)} \right| \; I=1/2, I_3=1/2 \right\rangle \tag{2.4b}$$

and the excellent approximation (to within 2%) that the decay momentum is the same for all channels, the ratio (2.2) takes the form:

$$\frac{|f_{3/2}|^2}{|f_{1/2}|^2 + |f_{3/2}|^2} \approx \frac{1}{982} \tag{2.5}$$

This result engenders the suspicion that the $\Delta I = 1/2$ channel is strongly enhanced relative to the $\Delta I = 3/2$ modes. To say that the $\Delta I = 1/2$ channel dominates is equivalent to assuming that the pions would prefer to be in a final state which has $I = 0$. If we assumed that $I = 0$ were the only possible final state, then we would find that:

$$\Gamma(K^0 \to \pi^0 \pi^0) = \frac{1}{2} \Gamma(K^0 \to \pi^+ \pi^-) \tag{2.6}$$

which is in good agreement with the experimental ratio 0.46 ± 0.01 .

It has long been believed, but not demonstrated, that the $\Delta I = 1/2$ enhancement is somehow due to QCD effects. Because the effect is so big, there is a reasonable hope that we could attempt to calculate the ratio from first principles. We should not expect to get the correct answer to within a few percent; however, we could expect to see the enhancement qualitatively at perhaps the 50% level.

Many attempts have been made to calculate the ratio (2.2); however, all such attempts have foundered upon the calculation of the hadronic matrix elements. At best, partially successful attempts have been made within the context of perturbative QCD [2]. More recently, the problem has been attacked using numerical lattice techniques in conjunction with chiral perturbation theory [3]. The final results for these calculations are not yet available. The hopping parameter expansion is also being considered by one group [4].

The Feynman diagrams involved in calculating the $K \to \pi\pi$ amplitudes are laid out in Fig.1. The gluon exchanges have been omitted because there are no particular gluon exchanges that we expect to be dominant; instead, all gluon interactions must be considered.

We presume that $\Delta I = 1/2$ is a general rule which will find application beyond K decays. Indeed, similar enhancements and suppressions are seen in the decays of the charmed mesons D and F, and in the decays of some strange baryons [5]. All these phenomena are good candidates for calculation by the methods we will employ here; especially those cases for which most of the quarks involved are heavy in which case the Strong Coupling Expansion should be more reliable. However, we will continue to work with the Kaon system because it is the best known, and cleanest case.

3 : The Strong Coupling Expansion

As Quantum Chromodynamics (QCD) became widely accepted as the best theory for describing the strong interactions, it was realized that the perturbative techniques of Feynman diagrams would be of no use for calculating the low energy and static properties of the theory. Hence, the following curious situation has arisen. There is a vast wealth of experimental results detailing the low energy regime of QCD, i.e., masses, magnetic moments, cross sections, and decay rates; however, owing to the mathematical complexity of the theory, we have only been able to calculate anything in the region of very high energies and momentum transfers. Although such results from "Perturbative QCD" have been of great utility, in any real experiment the low energy properties of QCD always manifest themselves so making a direct comparison of theory and experiment extremely difficult, if not impossible. To make any progress many phenomenological assumptions have had to be introduced but, despite heroic efforts, such features as the mass spectrum and hadronic matrix elements in the low energy regime have remained out of reach. As one of several attempts to solve this problem the Strong Coupling Expansion was introduced [6–8]. Here, we present a lightning review of the Strong Coupling Expansion as applied to QCD.

3.1. Introduction to Strong Coupling

The essential observation is that at infinite coupling lattice QCD is a free field theory and is exactly solvable. With the lattice providing all needed regulation of potential ultraviolet divergences we can perturb away from the infinite coupling limit using some form of perturbation theory. Two possible approaches to the Strong Coupling Expansion method have been advocated:

1) **Euclidean Lattice QCD :** Both time and space coordinates are discrete. Recently, for most calculations, this has been the preferred formalism. Its main advantage is the existence of a continuous chiral symmetry when Kogut–Susskind fermions are used. This formalism is also more easily adapted to numerical calculations with Monte Carlo methods.

2) **Hamiltonian Lattice QCD :** The space coordinates are discrete; however, time is now continuous. In this formulation the physical interpretation of calculated results is usually more direct than for the Euclidean theory. However, there is no continuous chiral symmetry so the details of the the promotion of discrete to continuous chiral symmetry are major issues of concern. Roughening tends to be less of a problem in this formalism; however, it will still appear in some contexts[9].

The Strong Coupling Expansion has been used in many contexts in statistical mechanics as a high temperature expansion; however, for QCD application has been sparse mainly because of the difficulty, and sometimes necessity, of calculating to high orders in perturbations from the infinite coupling limit. In Chap.4. we will describe how the Strong Coupling Expansion can be, and was, implemented on a computer as a specialized computer algebra system.

3.2. The Hamiltonian Formulation

The lattice theory of QCD that we are going to use is a Hamiltonian formulation with Kogut–Susskind fermions[8][10] which we shall describe shortly. The Hamiltonian for this system, with SU(N) local gauge symmetry, is:

$$H = \frac{g^2}{2a}(H_0 + H_1) + \text{H.C.} \tag{3.2.1a}$$

$$H_0 = \sum_{\text{links}} E^2 + \sum_f m_f \sum_{r,n} :\chi^\dagger{}_{fa}(r)\chi_f{}^a(r):(-1)^{x+y+z} \tag{3.2.1b}$$

$$+ \sum_f A_f \sum_{r,n} [\rho_f(r)\rho_f(r+n) + N^2]$$

$$H_1 = -\frac{1}{g^4}\sum_{\text{plaq}} Tr[UUUU] \tag{3.2.1c}$$

$$+ \frac{1}{g^2}\sum_{f,r,n} \eta_n(r)\chi^\dagger{}_{fa}(r)\,U^a{}_b(r,n)\chi_f{}^b(r+n).$$

$U^a{}_b(r,n)$ is the link variable, on the link $(r,r+n)$, representing the gauge fields and the E^2 are the quadratic Casimir operators on the links. The $\chi_f{}^a(r)$ are the fermion variables belonging to the generation labeled by f. They satisfy the anticommutation relations:

$$\{ \chi_f{}^a(r) , \chi_{f'}{}^{a'}(r') \} = \{ \chi^\dagger{}_{fa}(r) , \chi^\dagger{}_{f'a'}(r') \} = 0 \tag{3.2.2a}$$

$$\{ \chi_f{}^a(r) , \chi^\dagger{}_{f'a'}(r') \} = \delta^a{}_{a'}\,\delta_{ff'}\,\delta_{r\,r'} \tag{3.2.2b}$$

The operator ρ_f is defined by:

$$\rho_f(r) = [\, \chi^\dagger{}_{fa}(r) , \chi_f{}^a(r) \,] \tag{3.2.3}$$

The phases $\eta_n(r)$ are defined below in (3.3.12). The significance of the arbitrary constants A_f will be discussed in Sec. 3.5. Notice that the mass term in (3.2.1b) has been normal ordered. We will have more to say about this both in Sec.3.5., and in Chap.6. There is no necessity to normal order any of the other operators.

3.3. Kogut Susskind Fermions

In this section we construct the Hamiltonian for the fermions so that we can see how it relates to the continuum Hamiltonian. We also need to establish the sign conventions that we will use in all subsequent calculations.

The continuum Dirac equation, with the definition $\alpha^i = \gamma^0\gamma^i$, is:

$$\partial_t\psi + \alpha^i\nabla_i\psi = 0 \tag{3.3.1}$$

The gamma matrices have the following usual definitions:

$$\gamma^t = \begin{bmatrix} I & 0 \\ 0 & -I \end{bmatrix} \qquad \gamma^i = \begin{bmatrix} 0 & \sigma^i \\ -\sigma^i & 0 \end{bmatrix} \qquad \gamma_5 = \begin{bmatrix} 0 & I \\ I & 0 \end{bmatrix} \tag{3.3.2}$$

The σ^i are the standard Pauli spin matrices.

Our main task is to get around the "doubling" problem in some way. Following the method of Susskind [10], we place a single fermion ψ at each site on the lattice. We then subdivide the lattice into four sublattices as in Fig.2., identify the fermion field at, e.g., a "two" site to be the second component of a four component "spinor", and then simply postulate the equation of motion for the fermion field to be:

$$\partial_t\psi + \alpha^i\Delta_i\psi = 0 \tag{3.3.3}$$

or, in expanded form:

$$\partial_t\psi_1 + \Delta_x\psi_4 - i\Delta_y\psi_4 + \Delta_z\psi_3 = 0 \tag{3.3.4a}$$

$$\partial_t\psi_2 + \Delta_x\psi_3 + i\Delta_y\psi_3 - \Delta_z\psi_4 = 0 \tag{3.3.4b}$$

$$\partial_t\psi_3 + \Delta_x\psi_2 - i\Delta_y\psi_2 + \Delta_z\psi_1 = 0 \tag{3.3.4c}$$

$$\partial_t\psi_4 + \Delta_x\psi_1 + i\Delta_y\psi_1 - \Delta_z\psi_2 = 0 \tag{3.3.4d}$$

With lattice spacing a , the finite difference operators are defined by:

$$\Delta_z \psi \;=\; \frac{1}{2a}\left[\,\psi(r+n_z) - \psi(r-n_z)\,\right] \tag{3.3.5}$$

While four degrees of freedom are visible in this equation, in momentum space we will find eight independent fields at long wavelengths; hence, we will further subdivide the lattice. For even y coordinate, we denote the spinor ψ by f , and for odd y , ψ becomes g now giving us a total of eight fields. These have the equations of motion:

$$\partial_t f \;+\; \left[\,\alpha^x \Delta_x + \alpha^z \Delta_z\,\right] f \;+\; \alpha^y \Delta_y\, g \;=\; 0 \tag{3.3.6a}$$

$$\partial_t g \;+\; \left[\,\alpha^x \Delta_x + \alpha^z \Delta_z\,\right] g \;+\; \alpha^y \Delta_y f \;=\; 0 \tag{3.3.6b}$$

We now define two new spinors, u and d , by

$$u \;=\; (\,f \;+\; g\,)\;, \qquad\qquad d \;=\; -\,i\,\gamma_5 \gamma^y\,(\,f \;-\; g\,) \tag{3.3.7}$$

In component form, the u , d fields are related to the f , g fields by :

$$u_i \;=\; f_i \;+\; g_i; \qquad i \;=\; 1 \ldots 4, \tag{3.3.8a}$$

$$d_1 \;=\; f_2 \;-\; g_2, \qquad d_2 \;=\; g_1 \;-\; f_1,$$

$$d_3 \;=\; g_4 \;-\; f_4, \qquad d_4 \;=\; f_3 \;-\; g_3, \tag{3.3.8b}$$

With the two definitions of (3.3.7), the equations (3.3.6) become:

$$\partial_t u \;+\; \alpha^i \Delta_i u \;=\; 0 \tag{3.3.9a}$$

$$\partial_t d \;+\; \alpha^i \Delta_i d \;=\; 0 \tag{3.3.9b}$$

Hence, we see that the postulated equations of motion (3.3.2) turn out to be

equivalent to those of two independent spinors which have been suggestively named u and d. Indeed, in the long wavelength continuum limit we identify these fields as the two quarks of the same names.

Now that we have come this far, we move in the opposite direction from the original postulated field equations (3.3.3) to reach the convenient form of the Hamiltonian that was presented in (3.2.1b). Writing the equations in terms of the single fermion field at each site, denoted by ψ , the equations of motion (3.3.3) collapse to:

$$\begin{aligned} &\partial_t\psi \;+\; \frac{1}{2a}[\,\psi(r+n_x)-\psi(r-n_x)\,] \\ &\quad -\; \frac{i}{2a}[\,\psi(r+n_y)-\psi(r-n_{y)}\,](-1)^{x+y} \\ &\quad +\; \frac{1}{2a}[\,\psi(r+n_z)-\psi(r-n_z)\,](-1)^{x+y} \;=\; 0 \end{aligned} \tag{3.3.10}$$

Before proceeding, we need to make the definitions:

$$D(a,b) \;=\; \frac{1}{2}[1+(-1)^a+(-1)^b+(-1)^{a+b+1}] \tag{3.3.11a}$$

$$A(a) \;=\; \frac{1}{\sqrt{2}}[i^{a-\frac{1}{2}} \;+\; (-i)^{a-\frac{1}{2}}\,] \tag{3.3.11b}$$

These constructs will be used very frequently and have the useful properties:

$$D(a,b)^2 = 1, \qquad D(a,b)D(a+1,b) = (-1)^b \tag{3.3.12a}$$

$$A(a)^2 = 1, \qquad A(a)A(a+1) = (-1)^a \tag{3.3.12b}$$

We now make the field redefinition to define $\chi(r)$:

$$\psi(r) \;=\; (-i)^{x+z}A(y)D(x,z)\chi(r) \tag{3.3.13}$$

With this definition, the equation of motion we obtain is:

$$\partial_t \chi(r) - \frac{i}{2a}[\,(\chi^\dagger(r+n_x)+\chi(r-n_x))(-1)^z + (\chi^\dagger(r+n_y)+\chi(r-n_y))(-1)^x + (\chi^\dagger(r+n_z)+\chi(r-n_z))(-1)^y\,] = 0 \tag{3.3.14}$$

And so finally, the Hamiltonian which we can derive from (3.3.14) comes into view:

$$H = \frac{1}{2a}\sum_r [\,\chi^\dagger(r)\chi(r+n_x)(-1)^z + \chi^\dagger(r)\chi(r+n_y)(-1)^x + \chi^\dagger(r)\chi(r+n_z)(-1)^y + \text{H.C.}\,] \tag{3.3.15}$$

The phases $\eta_n(r)$ of (3.2.1c) can be read off immediately.

The symmetries of (3.3.15) are detailed in Appendix A: Table A.1. The main caveat is to be very careful about signs.

3.4. SU(4) Flavor Symmetry

Because we have incorporated two generations of fermions we might wonder if some remnant of the SU(4) flavor symmetry survives on the lattice. It does, and later on this will turn out to have great utility. Some details of this remnant symmetry are presented in Appendix A. The only symmetry operation that we will explicitly need is that of interchange of the fields of the two generations, denoted by T^1. We should keep in mind that this extended flavor symmetry is broken by both the mass terms and the four–fermion operators quadratic in ρ_f.

We must also point out that the SU(2) transformations within the two generations are not independent. A transformation that translates a fermion field by

one link, for example, must also carry the link gauge field with it. By this mechanism, the transformations for each individual generation are kept in lockstep. This has the unpleasant consequence that there is no such symmetry as "nuclear" isospin, henceforth denoted by I_N, for which only the u and d quarks have nontrivial transformation properties. There is however a "weak" isospin I_W under which all flavors transform simultaneously.

3.5. The Vacuum

For a single generation the vacuum state of the theory is defined by:

$$E^2 \mid 0_{glue}, \Psi_{ferm} \rangle = 0, \tag{3.5.1a}$$

$$\chi_f^a(r) \mid \Phi_{glue}, 0_{ferm} \rangle = 0, \quad x+y+z \text{ even}, \tag{3.5.1b}$$

$$\chi^\dagger_{fa}(r) \mid \Phi_{glue}, 0_{ferm} \rangle = 0, \quad x+y+z \text{ odd}, \tag{3.5.1c}$$

There are several points that need to be made regarding the way the vacuum state is defined for fermions. If the mass term for a particular generation is absent in (3.2.1b), then the theory has a discrete chiral symmetry. However, this symmetry is broken by the fermion vacuum which we choose to be:

$$\rho_f(r) \mid \Phi_{glue}, 0_{ferm} \rangle = -(-1)^{x+y+z} N \mid \Phi_{glue}, 0_{ferm} \rangle \tag{3.5.2}$$

Now we can understand the reason for including the term $A \sum \rho(r)\rho(r+n)$ in (3.2.1b). In the absence of a mass term, the vacuum for the fermion fields is totally degenerate. Much of this degeneracy is accidental and is not related to any symmetry of the Hamiltonian. In second order the interactions generate terms, of exactly this form, that lift almost all this degeneracy so that only two possible

vacuum states per generation remain; the state defined in (3.5.2), and another which is shifted by one lattice spacing relative to it. Another reason for including the final operator in (3.2.1b) is to ensure that, at least in the strong coupling limit, meson states constructed from baryon–antibaryon pairs have higher energies than the corresponding meson which spans a single link [8]. Because this operator is irrelevant, it will not affect any results in the continuum limit; however, in the strong coupling regime the presence of this term is a real nuisance.

If we have a fermion mass term for any given generation then we will continue to define the vacuum as in (3.5.1) and (3.5.2). From the definition (3.2.1b), we obtain the commutation relations:

$$[\, H_0 \,,\, \chi^a(r) \,] \;=\; -m(-1)^{x+y+z}\chi^a(r) \tag{3.5.3a}$$

$$[\, H_0 \,,\, \chi^\dagger{}_a(r) \,] \;=\; m(-1)^{x+y+z}\chi^\dagger{}_a(r) \tag{3.5.3b}$$

The normal ordering is defined by:

$$:\chi(r)\chi^\dagger(r): \;=\; -\chi^\dagger(r)\chi(r) \;, \qquad x+y+z \quad \text{even} \tag{3.5.4a}$$

$$:\chi^\dagger(r)\chi(r): \;=\; -\chi(r)\chi^\dagger(r) \;, \qquad x+y+z \quad \text{odd} \tag{3.5.4b}$$

otherwise, the ordering of the operators is unaffected. These definitions may seem counterintuitive; however, they are exactly what is required to ensure that the vacuum expectation of H_0 vanishes.

With two generations of fermions, there is another issue to address[11]. For the second generation, the definition of the vacuum in (3.5.2) could be as in (3.5.2) or there could be an additional minus sign, so the definition of the vacuum becomes:

$$\rho_1(r)\ |\Phi_{glue},0_{ferm}\rangle\ =\ -(-1)^{s_1}(-1)^{x+y+z}N\ |\ \Phi_{glue},\ 0_{ferm}\rangle \tag{3.5.5a}$$

$$\rho_2(r)\ |\Phi_{glue},0_{ferm}\rangle\ =\ -(-1)^{s_2}(-1)^{x+y+z}N\ |\ \Phi_{glue},\ 0_{ferm}\rangle \tag{3.5.5b}$$

were s_1 , s_2 equal zero or unity. If $s_1 \neq s_2$, then we can immediately show that the discrete SU(4) symmetry is broken by the vacuum. If $s_1 = s_2$, then this symmetry survives. Our problem is to decide which vacuum to use. For reasons of simplicity, and no other good reason, we choose the vacuum with the unbroken SU(4) flavor symmetry.

3.6. Rayleigh–Schroedinger Perturbation Theory

In the Hamiltonian formalism, the theory we have looks like what we are familiar with from standard quantum mechanics; hence, we will use Rayleigh–Schroedinger perturbation theory which we briefly summarize here [12]. For simplicity, we shall assume that there are no troublesome degeneracies. All of our calculations will be based on the expressions:

$$|\psi\rangle\ =\ |\psi_0\rangle + \frac{Q}{E - H_0} V\,|\psi\rangle \tag{3.6.1a}$$

$$H_0|\psi_0\rangle\ =\ E_0|\psi_0\rangle \tag{3.6.1b}$$

$$H\,|\psi\rangle\ =\ E\,|\psi\rangle \tag{3.6.1c}$$

$|\psi_0\rangle$ is the unperturbed state and is normalized to unity, $|\psi\rangle$ is the corresponding unnormalized eigenstate of the full Hamiltonian, and Q is the operator that projects out the subspace orthogonal to the state $|\psi_0\rangle$. The energy of a given perturbed state, with the vacuum energy not subtracted, is given by:

$$E - E_0 = \langle \psi_0 | V | \psi \rangle \tag{3.6.2}$$

For weak interaction matrix elements we will need to evaluate:

$$\frac{\langle \psi^{(2)} | H_W | \psi^{(1)} \rangle}{\langle \psi^{(2)} | \psi^{(2)} \rangle^{1/2} \langle \psi^{(1)} | \psi^{(1)} \rangle^{1/2}} \tag{3.6.3}$$

$|\psi^{(1)}\rangle$, $|\psi^{(2)}\rangle$ are both eigenstates of the full Hamiltonian (up to some order in strong coupling). Notice that here we have to worry about normalizing the wave function. This normalization performs the important task of removing all terms in the numerator which are derived from vacuum bubbles and have coefficients that depend on the size of the lattice.

We then proceed to iterate these expressions so that all matrix elements are expressed entirely in terms of the unperturbed wave functions. The first few terms in these expansions are:

$$E - E_0 = \langle \psi_0 | V | \psi_0 \rangle + \langle \psi_0 | V \frac{Q}{(E - H_0)} V | \psi_0 \rangle + \cdots \tag{3.6.4a}$$

$$\langle \psi^{(2)} | H_W | \psi^{(1)} \rangle = \langle \psi_0^{(2)} | H_W | \psi_0^{(1)} \rangle \tag{3.6.4b}$$

$$+ \langle \psi_0^{(2)} | V \frac{Q}{(E_2 - H_0)} H_W | \psi_0^{(1)} \rangle + \langle \psi_0^{(2)} | H_W \frac{Q}{(E_1 - H_0)} V | \psi_0^{(1)} \rangle + \cdots$$

$$\langle \psi | \psi \rangle = 1 + 2 \langle \psi_0 | V \frac{Q}{(E - H_0)^2} V | \psi_0 \rangle + \cdots \tag{3.6.4c}$$

In a real calculation there is a remaining complication; the energy denominators are expressed in terms of the exact energy rather than the unperturbed energy, so making the equations very difficult to deal with. Expanding E, and the energy denominators, we get:

$$E = E_0 + \sum_p^{\infty} \frac{\varepsilon_p}{g^{2p}} \tag{3.6.5a}$$

$$\frac{1}{(E - H_0)} = \frac{1}{(E_0 - H_0)} \tag{3.6.5b}$$

$$+ \sum_{n=1}^{\infty} (-1)^n \frac{1}{(E - H_0)^{n+1}} [\sum_p^{\infty} \frac{\varepsilon_p}{g^{2p}}]$$

Although this is messy to do by hand, it is trivial for a computer. It is important to remember that E contains a contribution from the vacuum energy and so the ε_p contain pieces which are proportional to the size of the lattice. These terms are removed when we subtract, order by order, the vacuum energy from (3.6.2), or when we divide by the wave function normalization as in (3.6.3).

One point we need to make is that whenever the unperturbed state appears as an intermediate state in (3.6.5) the energy denominator vanishes, therefore these terms must be neglected from the sum. An important advantage of the computer algebra approach to this problem is that the energy denominators are evaluated exactly; hence, we may easily identify the terms that must be ignored.

3.7. Generalizations

Some final comments that should be made are that the Hamiltonian we have chosen (3.2.1) to use here is the simplest we can escape with. We could have included additional magnetic terms using SU(N) matrices with indices which transform as higher representations of the gauge group, and terms based on six, or more, link operators [13]. At present, such additions would appear to be increasing complication without obviously improving the results that we will get, therefore we will take heed of "Ocam's Razor" and proceed with (3.2.1). Such generalizations might come in useful if we had to maneuver around a singularity as

we extrapolate to the continuum limit. Also, we have chosen the quarks within any generation to be degenerate. We could split these states, but it is an unpleasant procedure and involves operators which span two links on the lattice (see the form of $\overline{\psi}\tau_3\psi$ in Appendix A). How to construct perturbation theory for this particular case is unclear.

3.8. Monte Carlo Methods

Over the last decade, most attempts to understand the low energy phenomenology of QCD from first principles have focused on the use of Monte Carlo techniques to directly evaluate the path integral. While such methods have enjoyed some success, one is left with the feeling that the computer knows more about what physics was included than you do. An analytic technique would be preferable if it would provide us with some insight to the relevant physics. It is in this regard that the use of computer algebra has great promise. Also, strong coupling has two major advantages over the use of numerical methods; we are able to use infinite lattices, so boundary effects are not a concern, and we are not at the mercy of round off errors and statistical fluctuations. The main drawback with the method is the need to use padé approximants or some other scheme of extrapolating to the continuum limit. This extrapolation is, of course a severe problem for Monte Carlo methods as well. In fact, that the continuum limit really exists for these cases is something of an article of faith. Finally, the fear of any type of phase transition between the weak and strong coupling regimes must be considered in either scheme.

A useful discussion of many of the methods that have been used in the context of lattice gauge theories is presented in [14].

4 : Strong Coupling and Computer Algebra

As was mentioned in the previous section, a major reason why the Strong Coupling expansion has not been used extensively for practical calculations is the complexity of higher orders. This suggests the possibility of writing a specialized computer algebra package to aid in doing calculations. The ultimate computer program designed to do strong coupling calculations would simply accept as input the initial and final states, and perhaps the form of a weak interaction Hamiltonian, and then would grind away until (perhaps in near infinite time!) it had constructed all relevant graphs and then evaluated them.

The design and implementation of this program are the subject of this section. In Fig.3. an overview of a Strong Coupling computer system is given. The subsections of this chapter essentially follow the elements of Fig.3. For simplicity, much of our discussion will be confined to the pure gauge situation.

4.1. Graph Construction

4.1.1. Graph Construction and Computational Equivalence

The hardest aspect of building such a program is the construction of the graphs. The computer needs to be able to recognize when two configurations, which it has constructed via different routes, are identical up to translations and/or rotations. For our purposes, a simplified and yet complete system was written. At a given order P in perturbation theory the number of distinct graphs, before time ordering and complex conjugation (see next section) are implemented, is of the order of:

$$\#_{Graphs} \approx 3^{P/2} \prod_{i=0}^{\frac{P}{2}-1} (4+3i) \tag{4.1.1}$$

The salient point to remember from (4.1.1) is the exponential factors. The second, and technically more difficult, feature we require is the ability to recognize when two distinct configurations are computationally equivalent, i.e., they evaluate to the same number. This is important because the calculation of an individual graph can be an expensive thing to do for SU(N) and there are many calculationally equivalent graphs. As a comparison, for a Z_2 gauge theory (in the Euclidean formulation) we would not have to worry as much because the evaluation of graphs is so much easier.

4.1.2. Time Ordering and Complex Conjugation

To obtain all of the graphs, the remaining steps we have to execute are to time order all of the perturbations, and then construct all possible orientations (defining whether we have taken the perturbation, or its complex conjugate) of the plaquette/fermion–Hamiltonian perturbations within a graph. These steps are easy to implement and it is mainly these steps which are responsible for the very large number of graphs which we must consider even for quite simple situations. For any given graph of even order P, time ordering will contribute distinct configurations enumerated by:

$$\#_{Time\ Orders} \approx \frac{P!}{2^{P/2}} \tag{4.1.2}$$

The dividing factor appears because, ignoring all possible orientations, we usually need identical pairs of perturbations to ensure a nonvanishing graph. (4.1.2) is worst case behavior; of course, some diagrams have only a single time ordering. For each individual time ordering, the various possible orientations of the

perturbations will contribute of the order of:

$$\#_{Orientations} \approx \frac{1}{2}\prod_{c}\frac{(P+2)!}{[\,(\frac{P}{2}+1)!\,]^2} \tag{4.1.3}$$

graphs. c labels the independent sets of links within a graph. The overall factor of one half arises because we can fix the orientation of the initial *or* final state if one so wishes. For SU(N), with N odd, (4.1.2) is a slight underestimate.

For SU(2) we do not need to construct distinct graphs for the orientations of plaquettes; however, for the reasons of ease of programming it is advantageous to have assigned orientations. This is because the computer algebra program is very specific about indices being correctly placed up or down, which is equivalent to having an assigned orientation.

4.1.3. Disconnected Graphs and Splicing

From a purely theoretical point of view, Rayleigh–Schroedinger perturbation theory is an extremely inefficient procedure. There are many disconnected graphs and it would therefore seem that we would calculate many graphs more than once. Unfortunately, "linked cluster" expansions are only known to exist for special cases [15]. However, it turns out that the situation is not as grim as it might appear; in principle, we need only compute the connected graphs and then we may form the disconnected graphs by splicing them together. Most of the work involved in splicing two graphs together comes from constructing the time orderings and evaluating the energy denominators. This procedure is recursive and fits naturally into the process of working from lower to higher order.

The calculation of the excluded volume coefficients, while straightforward in simple cases, gets to be very difficult in higher order. This calculation is also

recursive in the number of disconnected pieces. Development of an efficient algorithm and computer code which can calculate these coefficients quickly will be necessary if very high order calculations are ever to be attempted. Such algorithms will be of the same level of complexity as those employed for the construction of the basic graphs. A program was developed for this purpose; however, except for the simplest cases it proved to be cumbersome to use. At present, the excluded volumes are simply tabulated and called when needed.

4.2. The Group Theory

4.2.1. Gauge Field Expectation Values

Having constructed the graphs at a particular order in perturbation theory we must now write down the corresponding mathematical expressions and then evaluate them. Most of the labor lies in the evaluation of the expectation values of SU(N) link variables. Generically we have:

$$\langle 0 \mid \cdots U^{a}{}_{a'}(r,n) \cdots U^{\dagger b'}{}_{b}(r,n) \cdots \mid 0 \rangle \tag{4.2.1}$$

$$= \int d\mu_G [\, \cdots U^{a}{}_{a'} \cdots U^{\dagger b'}{}_{b} \cdots \,]$$

The unprimed indices correspond to the coordinate r, the primed indices to the $r+n$ end of the link. Evaluation of this integral is, in principle, straightforward via the Clebsch–Gordon coefficients. Two tricks enable us to do these calculations easily on a computer and in such a way that we can easily modify our programs to use a group other than SU(3), to which we now specialize. The modification to SU(2) has been implemented but will not be employed here.

The first thing to do is to keep all indices in the fundamental representation 3, and its conjugate $\overline{3}$; hence, a 6 will be represented as $\phi^{(ab)}$ with the a, b indices symmetrized. Whenever two indices are antisymmetric, we use the antisymmetric symbol to reduce the two indices to one, i.e.,

$$\phi_a = \frac{1}{\sqrt{2}} \varepsilon_{abc} \phi^{[bc]}. \tag{4.2.2}$$

This method is general enough that inclusion of news terms in the Hamiltonian, such as characters of higher representations, could be incorporated without too much difficulty.

We also notice that any given term in the expectation value factorizes into a tensor which exhibits only unprimed indices, and a primed index tensor which has the identical structure except that the complex conjugate has been taken. An example is provided in (4.2.4). The reason for this factorization is that our gauge transformations are local, so we cannot have indices corresponding to different space points in the same tensor. Hence, it is enough for us to construct one of these tensors, and then the other may be immediately written down.

We proceed by simply working along the SU(3) matrices in (4.2.1) from left to right. At each step we take the current representation, construct its group product with a 3 (or $\overline{3}$ if we have a $U^\dagger$) and then decompose to the irreducible representations using the tensor method, e.g.,

$$3 \otimes \overline{3} = 8 \oplus 1 \tag{4.2.3a}$$

$$\phi^a \phi_b = P^a{}_b{}^n{}_m [\phi^m \phi_n] + \frac{1}{3} \delta^a{}_b [\phi^m \phi_m] \tag{4.2.3b}$$

$$P^a{}_b{}^n{}_m = \delta^a{}_m \delta^n{}_b - \frac{1}{3} \delta^a{}_b \delta^n{}_m \tag{4.2.3c}$$

The tensors $P^{a}{}_{b}{}^{n}{}_{m}$ and $\delta^{a}{}_{b}$ give us the Clebsch–Gordon coefficients up to a normalization which we must determine. This is the only hard part of the calculation. The easiest method to use is to recall that Clebsch–Gordon coefficients are unitary; hence, we find that the coefficients for this example are 1 and $1/\sqrt{3}$. Therefore, an example of an expectation value is:

$$\left\langle 0 \mid U^{a}{}_{a'} U^{\dagger b'}{}_{b} U^{m}{}_{m'} U^{\dagger n'}{}_{n} \mid 0 \right\rangle \tag{4.2.4}$$

$$= \frac{1}{8} P^{a}{}_{b}{}^{m}{}_{n} P^{b'}{}_{a'}{}^{n'}{}_{m'} + \frac{1}{9} \delta^{a}{}_{b} \delta^{m}{}_{n} \delta^{b'}{}_{a'} \delta^{n'}{}_{m'}$$

The Clebsch–Gordon coefficients that would be required to handle an arbitrary calculation involving up to six coincident links are tabulated in Appendix C. To date, the system can accommodate up to eight links.

Currently, evaluating the Clebsch–Gordan coefficients is done by hand but in the future it will be computerized. There is one technical point which one needs to be aware of, namely that two representations may have the same dimension and yet not be equivalent. The only example we encounter is:

$$10 \otimes 3 = 15_1 \oplus 15_2. \tag{4.2.5}$$

These inequivalent 15 representations have different symmetry properties and different quadratic Casimir operators. The magnitudes of the different Casimir operators are given in Appendix C: Table (C.3).

Finally, it is much more efficient to compute all of these coefficients ahead of time and then call the results when needed in any particular calculation of a graph. This requires a method of uniquely identifying any particular configuration of U and $U^{\dagger}$ matrices. This is almost trivial; by assigning 1 to U and -1 to a $U^{\dagger}$, we use the hashcoding H defined by:

$$H = \sum_{p=1}^{Q} (\pm 1) 3^p \tag{4.2.6}$$

where the sum is over the Q SU(3) matrices that are present. The number of possible expectation values increases very rapidly, for large Q being bounded above by $(Q/2)!$ Above six matrices is impossible by hand, with six matrices being just tolerable.

4.3. Evaluation of the Graphs

4.3.1. Computer Algebra

This short program is the heart of the entire system. While the basic algorithm used is very general, for speed and economy of memory usage, the code has been specialized to handle just three mathematical constructs; they are the invariant tensors of SU(3) ; ${\delta^a}_b$, $\varepsilon^{a_1 \cdots a_N}$, and $\varepsilon_{a_1 \cdots a_N}$. A very similar program is also used for the calculation of the Clebsch–Gordon coefficients.

4.3.2. Fermion Expectation Values

The evaluation of the expectation values of a group of fermionic operators at a single site is almost trivial. We simply use the anticommutation relations (3.2.2) repeatedly.

Wilson fermions could be implemented; however, in that case we would have four Dirac fields per site (plus color indices). This makes the algorithms significantly more complicated. Also, the gamma matrices have to be accommodated. In part, the decision to use Kogut–Susskind fermions was based upon these reasons. The price we pay for this choice is the phases of the now distributed gamma matrices, and the absence of a nuclear isospin symmetry. Of these two the latter

is by far the more damaging.

4.4. Processing the Amplitudes

This can be easy, or very difficult, to do depending on the calculation under consideration and what kind of answer is required. If an answer with all arbitrary parameters left explicit is desired then this job can be very difficult; however, purely numerical answers do not provide a problem. In either case, a minimal amount of computing time is expended here.

4.5. Testing

With any computer program, there is the vexing question of how to test it. Here we very briefly indicate how the programs were tested.

It turns out that there are various consistency checks which can be made within any particular calculation. Most of the disconnected graphs derive from the vacuum bubbles. These terms have coefficients which have the form $a_p N^p + a_{p-1} N^{p-1} \cdots a_0$. The a_0 is the only term that will contribute to the final answer. The other terms, which are powers of N, have to cancel in the final analysis, order by order in strong coupling perturbation theory. These cancellations give a useful check on the results. If a string tension calculation is used as a check, then all terms of the form $N^p L^q$ must have vanishing coefficients when $p>0$ and $q>1$. Note that subdominant terms e.g., terms proportional to L^{-1} , need not vanish.

To check that the group theory has been done correctly, we evaluate the amplitude (ignoring the energy denominators for the moment) of a diagram for which the plaquettes coincide on the lattice. Due to the orthonormality of the Clebsch–Gordon coefficients these amplitudes must evaluate to unity. Although

this check is not foolproof, it gives us some confidence in our calculations. If one has a lot of nerve, then we can use this method to fix the normalizations of the Clebsch–Gordon coefficients.

A final, rather unreliable test was to check against the few published results available. The results were rather saddening with most of the calculations in the literature appearing to have errors. The pioneering glueball mass calculations of [7] are completely in error; despite which, the final results appear to be quite reasonable. The meson and baryon mass calculations of [8] also appear to have some minor errors. However, the string tension calculations [16] are the best, we tested up to fifth order in $3+1$ dimensions.

5 : Initial/Final State Wave Functions

Before attempting to construct the operators for the weak Hamiltonian, we will construct the wave functions for the initial and final states. This exercise will illustrate the methods that we will use. First, for pedagogical purposes we will construct the single pion state, then the Kaons, and finally, the two pion wave function.

5.1. Lattice Bilinears in General

To construct the fermion bilinear operators, and the quartic operators in Chap.6., we use the following method. In many cases we encounter we use lattice operators which are summed over all lattice sites; hence, we make the correspondence:

$$\int d^3x\, \overline{\psi}\Gamma\psi \;\rightarrow\; \sum_{r,i} \alpha_r{}^{(i)} \chi^{\dagger}(r)\chi(r+a^{(i)}) \;+\; \eta_c \text{ H.C.} \tag{5.1.1}$$

The $a^{(i)}$ are linear combinations of the unit lattice vectors. r runs over all lattice sites and i runs over the distinct $a^{(i)}$ which emanate from a given site r . η_c is positive or negative depending on whether $\overline{\psi}\Gamma\psi$ is hermitian or antihermitian. For simplicity, we have assumed that there is no explicit factor of i present in (5.1.1). Such a factor is not a problem in practice, except for the sign confusion that it can cause. We now require that this lattice operator have the same transformation properties under lattice symmetry operations as has the continuum operator under the equivalent continuum transformations. Operators do not always look as symmetric as one might expect owing to the arbitrary choice of whether χ or $\chi^{\dagger}$ is located at r. For the purposes of constructing the four-fermion operators, we exploit this ambiguity so as to construct operators for which the transformation law under space inversion is manifest. We write the

lattice operator (5.1.1) as:

$$\frac{1}{2}\sum_{r,i} \alpha_r{}^{(i)} \chi^\dagger(r)\left[\chi(r+a^{(i)}) + \eta_P \chi(r-a^{(i)})\right] \; + \; \eta_c \text{ H.C.} \tag{5.1.2}$$

where $\eta_P = \pm 1$ depending on the parity. The advantage of this format is that the local operator

$$B(r) \; = \; \frac{1}{2}\sum_{i} \alpha_r{}^{(i)} \chi^\dagger(r)\left[\chi(r+a^{(i)}) + \eta_P \chi(r-a^{(i)})\right] \; + \; \eta_c \text{ H.C.} \tag{5.1.3}$$

has definite parity and hermiticity properties. When we need to use the bilinear operator outside of a sum over the lattice, then (5.1.3) is the form that we must use; however, in many other circumstances, we will be able to use the simpler form (5.1.1). To find the $a^{(i)}$, write the continuum bilinear in terms of the u, d fields, then in terms of f, g spinors as was described in Sec. 3.3. Concentrating on those operators that involve f_1, one will obtain the overall phase and the $a^{(i)}$. To pin down the $\alpha_r{}^{(i)}$, we do not have to utilize all of the lattice operations. The chiral flavor symmetries will be sufficient to determine an $\alpha_r{}^{(i)}$ corresponding to a particular $a^{(i)}$ by relating it to the coefficients residing on adjacent sites. If necessary, to fix the phases between different $\alpha_r{}^i$, employ the combined rotations and isorotations on the lattice. With these prescriptions, a compendium of the fermion bilinears that we will need is presented in Appendix A.

There are rare, but important, situations for which we need to be a little more careful than we were above. If the offset a is zero then we can take the correspondence between lattice and continuum currents to be either of:

$$\int d^3x \, [\,\overline{\psi}\,, \Gamma\psi\,] \; \rightarrow \; \sum_r \alpha_r \rho(r) \tag{5.1.4a}$$

$$\int d^3x \, :\overline{\psi}\Gamma\psi: \; \rightarrow \; \sum_r \alpha_r :\chi^\dagger(r)\chi(r): \tag{5.1.4b}$$

In the continuum limit (5.1.4a) and (5.1.4b) are equivalent[17]; however, this equivalence fails for our lattice constructions. Using either form ensures that if a current's vacuum expectation value should vanish in the continuum limit, then it will do so when averaged over a unit cube. Note; however, for (5.1.4a) the expectation value will not vanish at an individual lattice site, but only when averaged over a unit cube. For the prescription of (5.1.4b) the vacuum expectation vanishes identically at every site. When we constructed H_0 in Chap.3. we found that only the prescription of (5.1.4b) was satisfactory in ensuring that the energy of the vacuum was zero. From now on we will use the prescription of (5.1.4b). Both prescriptions are trivially satisfied for the general case of a non-vanishing $a^{(i)}$.

While the above prescription is perfectly adequate for constructing bilinears within a single generation, it needs some modification for operators which contain fields from different generations. In this case we choose to extend from the form (5.1.2):

$$\int d^3x\, \overline{\psi}_1 \Gamma \psi_2 \;\rightarrow\; \tfrac{1}{2} \sum_{r,i} \alpha_r{}^{(i)} \{ \chi^\dagger{}_1(r) [\, \chi_2(r+a^{(i)}) + \eta_P \chi_2(r-a^{(i)}) \,] \qquad (5.1.5)$$

$$+\; \eta_{CS} [\, \chi^\dagger{}_1(r+a^{(i)}) + \eta_P \chi^\dagger{}_1(r-a^{(i)}) \,] \chi_2(r) \}$$

The difference between this bilinear and those above is that there is no hermitian conjugate piece to the operator; instead, we find something similar. What we require is a way to fix η_{CS} . The trick is to remember that all bilinears of this form belong to the adjoint representation of SU(4). This means that the complex conjugate operator to that in (5.1.2) can also be reached from (5.1.2) by an SU(4) transformation. Using this observation, we may fix the η_{CS} easily. We observe that, with the SU(4) transformation T^1 (see Appendix A) that interchanges the

generations, and with the definition $\gamma^0\Gamma^\dagger\gamma^0 = \eta_C\Gamma$:

$$C : \overline{\psi}_1\Gamma\psi_2 = \eta_C\overline{\psi}_2\Gamma\psi_1 \tag{5.1.6a}$$

$$T^1 : \overline{\psi}_1\Gamma\psi_2 = \overline{\psi}_2\Gamma\psi_1 \tag{5.1.6b}$$

and therefore $\eta_{CS} = \eta_C$ which was derived while working with only one generation of fermions.

5.2. An Example : A Single Pion

The continuum limit guess for the π^0 wave function is, in the usual notation and up to a normalization factor:

$$\pi^0 \approx i\overline{\psi}\gamma_5\tau_3\psi \mid 0\rangle \tag{5.2.1}$$

The prescription that we employ is to construct the appropriate fermion bilinear operator by the method described in Sec.5.1., and then to use this operator as an interpolating field to the state that we want to reach. With this prescription, we obtain for the π^0 wave function, in its simplest form:

$$\frac{1}{\sqrt{3}}\sum_r (-1)^{y+z}\left[\,\chi^\dagger{}_a(r)\chi^a(r+n_z) + \chi^\dagger{}_a(r+n_z)\chi^a(r)\,\right] \mid 0\rangle \tag{5.2.2}$$

We can immediately obtain the wave functions, π_1 and π_2 (corresponding to the flavor generators τ_1 and τ_2) by cyclic permutations and then construct the charged pions as

$$\pi^\pm = \pm\frac{1}{\sqrt{2}}\left(\,\pi_1 \pm i\,\pi_2\,\right) \tag{5.2.3}$$

These wave functions were chosen because they are eigenstates of the

Hamiltonian in the strong coupling limit, and they have the same quantum numbers as the pions. As one proceeds to the continuum limit, contributions from operators spanning more than one link, along with baryon–antibaryon pairs (which we have explicitly suppressed by using the irrelevant operators) will be mixed into the true wave function. The irrelevant operators serve the very convenient purpose of suppressing the effect of baryon–antibaryon pairs. If $A_1 < 1/84$ then the baryon–antibaryon pairs would be lighter than the meson wave function (5.2.2) and so we would be unable to use (5.2.2) [8]. We assume that the assumptions underpinning (5.2.2) are not too drastic.

5.3. The Initial State : The Kaons

The Kaons present us with some new problems which originate because we are now incorporating quarks from different Kogut–Susskind fields. However, we can still apply the logic that was used to construct the pions.

In the continuum language, consider the wave function $\bar{c}\,u - \bar{s}\,d$ which is the direct analog of the π^0 wave function in (5.2.1) and can be written as:

$$\frac{1}{2}\, i\, \overline{\psi}_a \gamma_5 [\, T^1{}_3 - i\, T^2{}_3]^a{}_b \psi^b \mid 0 \rangle \tag{5.3.1a}$$

$$= i\, \overline{\psi}_2 \gamma_5 \tau_3 \psi_1 \mid 0 \rangle \tag{5.3.1b}$$

Where the index a ranges over the two generations and the T matrices are those defined in Appendix A. Using (5.3.1b) this new wave function can be written as:

$$\frac{1}{2\sqrt{3}} \sum_r (-1)^{y+z} \Big\{ \chi^\dagger{}_{2a}(r) [\, \chi_1{}^a(r+n_z) \; - \; \chi_1{}^a(r-n_z) \,] \tag{5.3.2}$$

$$+ \; [\, \chi^\dagger{}_{2a}(r+n_z) - \chi^\dagger{}_{2a}(r-n_z) \,] \chi_1{}^a(r) \Big\} \mid 0 \rangle$$

By rearranging the terms in the sum, and removing all terms that vanish, we are able to collapse (5.3.2) to:

$$\frac{1}{\sqrt{3}} \sum_r (-1)^{y+z} \chi^\dagger{}_{2a}(r) [\chi_1{}^a(r+n_z) - \chi_1{}^a(r-n_z)] \mid 0\rangle \tag{5.3.3}$$

We notice that the field χ_2 only resides on even lattice sites and the χ_1 field on odd sites. Hence, the phase of $(-1)^{y+z}$ could effectively be replaced by $(-1)^x$. An important point to now notice is that we can no longer make any use of the chiral symmetries because they are broken by the vacuum. Similarly, we can construct wave functions using the T matrices to form the charged mesons; however, we will not need any of these wave functions.

If we are going to use (5.3.3) to represent the K^0 there is an important physical issue which must be addressed. The wave function that we wrote down in (5.3.3), i.e., $\bar{c}\,u - \bar{s}\,d$, represents a superposition of the K^0 and $\bar{D}^0$. To get rid of the unwanted $\bar{u}c$ part, we might be inclined to construct the operator $\bar{c}\,u + \bar{s}\,d$, or $\bar{\psi}_a \gamma_5 \psi^a$, and then take the difference of the two operators to eliminate the $\bar{c}\,u$ component. However, in the strong coupling limit, these two states have different energies because the point split operators traverse one and three links respectively. We shall choose (5.3.3), instead of $\bar{\psi}_a \gamma_5 \psi^a$, to be our representation of the K^0 because in the limit of $m_s \to 0$, this wave function and the pions become degenerate. We could expect that $\bar{c}\,u$ components would cause us plenty of trouble; however, in the matrix elements which we shall compute, the $\bar{c}\,u$ part will not contribute and we can simply ignore it.

The other major concern is that the wave function (5.3.2) does not have $I_N = 1/2$ because there are no nuclear isospin symmetries in this model. The closest we come is the weak isospin for which the state (5.3.2) has $I_W = 1$. It is not immediately obvious just how much trouble this will be. It will turn out to be

very annoying.

5.4. The Final State : Two Pions

The final state of the K decays we are interested in have two pions; hence, we need to construct a two pion wave function on the lattice. An important physical issue we need to address is that of final state interactions. This will be discussed shortly.

The obvious choice for the two pion state, at rest in the center of mass and ignoring isospin factors and normalizations, is:

$$\sum_{r_1 r_2} e^{ikr_1}\pi^0(r_1)\, e^{-ikr_2}\pi^0(r_2) \tag{5.4.1}$$

For our calculation, we will force $m_K = m_{\pi\pi}$, at least to lowest order, so we set k to be zero. $\pi^0(r)$ represents the operator that we use to represent a single pion straddling one link. Unfortunately, as it stands (5.4.1) is not an eigenstate of the zeroth–order Hamiltonian. We can isolate several distinct components from (5.4.1), each of which is an eigenfunction with a distinct energy. The configurations for which the pions do not coincide completely (this state has energy $\frac{4}{3} + 128A_1$) are depicted schematically in Fig.4. along with their energies.

The only possible wave function that reproduces the large scale form of the two pion wave function is:

$$\sum\nolimits'_{r_1 r_2} \pi^0(r_1)\,\pi^0(r_2) \tag{5.4.2}$$

where the sum over r_1, r_2 is restricted so that the pions never get closer than two links to each other. The other states appear to represent primarily $q\bar{q}q\bar{q}$ exotic states. As we progress to the continuum limit, presumably the true pion wave

function becomes a mixture of all of these possibilities. In a more elaborate calculation than we entertain here, one might attempt to mix these states together in the strong coupling limit using the methods of [18]. Happily, for all of these states, I_N and I_W coincide.

Which of these wave functions we choose to calculate with should be arbitrary; after all, the $\Delta I_N = 1/2$ rule is presumed to be a general feature of non-leptonic weak decays. (5.4.2) best reproduces the way the wave function of the two pions spreads over space; however, it does not do as good a job of dealing with final state interactions, at least at low order in strong coupling perturbations. For the convenience of calculation, we choose to use the wave functions of Fig.4(b). This choice will mean that we over-include the final state interactions.

The wave function we use, omitting the gauge fields, is:

$$(\pi^0\pi^0) = \left\{ \frac{1}{6}\sum_r \chi^\dagger{}_a(r)\chi^a(r+n_z)[\chi^\dagger{}_b(r+n_x+n_z)\chi^b(r+n_x) \right. \tag{5.4.3}$$

$$\left. - \chi^\dagger{}_b(r+n_y+n_z)\chi^b(r+n_y)] + \text{H.C.} \right\} | 0\rangle$$

This wave function has positive parity, and is real. The $\pi^1\pi^1$ and $\pi^2\pi^2$ states are formed trivially from (5.4.3) by using the cyclic permutation symmetry. The "direction" of these states on the lattice is defined by the axis along which the contractions over color indices is taken. The $I = 0$ and $I = 2$ states are obtained by forming the linear combinations of (2.3).

5.5. The Strange Quark Mass

It would be preferable if we were able to calculate the matrix elements of interest on shell. Unfortunately, due to the splitting of the two isospin states, this is not possible except at lowest order. We do not believe that this problem is critical. The best that we can hope to achieve is to fix one of the matrix elements to be on shell. To do this, we will have to finetune the mass of the s-quark mass so that $m_K = m_{\pi\pi}$. While for this calculation this is an expedient, that relieves us of having to use wave functions carrying nonzero momentum, it probably is not that poor an approximation given $m_K \approx 490 MeV$ and $m_\pi \approx 140 MeV$.

For the mass term representing the c , s generation, we define:

$$m_s = \frac{4}{3} + \sum_{r=1}^{\infty} m_s^{(r)} g^{-2r} \tag{5.5.1}$$

This term treats the c and s quarks as degenerate. In the strong coupling limit, the mass of the $\pi\pi$ state that we have chosen to use, and the K, are:

$$m_{\pi\pi} = \frac{8}{3} + 4m_u + 128A_1 \tag{5.5.2a}$$

$$m_K = \frac{4}{3} + m_s^{(0)} + m_u + 36A_1 + 36A_2 \tag{5.5.2b}$$

We see that to fix $m_K = m_{\pi\pi}$ to zeroth order, set

$$m_s^{(0)} = \frac{4}{3} + m_u \tag{5.5.3a}$$

$$A_2 = \frac{23}{9} A_1 \tag{5.5.3b}$$

We are permitted to relate the irrelevant parameters in any way that we choose because, as long as we keep them finite, they in principle do not affect the

continuum limit although they will affect the final answer that we obtain.

This is as much as we will have to say about the energies of the states as the zeroth order results are all that is needed. For the record, the splitting between the two isospin states is given by:

$$E_2 - E_0 = +\frac{1}{4\,g^4} \tag{5.5.4}$$

5.6. Wave Function Normalizations

We would expect that for a second order calculation, we would need to compute the masses and wave function normalizations to second order. However; because of some remarkable cancellations that will occur, we will only need the zeroth order results. In particular, we only need the zeroth order normalization for the initial and final state wave functions. Because these will divide out of any ratio, we will drop these extraneous factors forthwith.

6 : The Weak Interaction Hamiltonian

The purpose of this section is to construct, on the lattice, the effective weak interaction Hamiltonian. If we were very ambitious, we might attempt to place the full Weinberg–Salam theory on the lattice and then calculate; however, this would be unnecessarily complicated. Instead, we will derive an effective theory in the continuum limit and then transfer to the lattice.

6.2. The Continuum Hamiltonian

In general, the hadronic matrix elements that we wish to calculate have the form [3]:

$$\int d^4x \int d^4y \, \langle \beta \mid T[J^\mu(y+\tfrac{1}{2}x)J^\nu(y-\tfrac{1}{2}x)] \mid \alpha \rangle D_{\mu\nu}(x, M_W) \qquad (6.1.1)$$

$|\alpha\rangle$ and $|\beta\rangle$ are hadronic states. Because the W mass is large relative to the scales which we are interested in, we can obtain an effective Hamiltonian by utilizing the Operator Product Expansion. At (or just below) the scale of the weak interactions, which we take to be M_W, the W–exchange term in this Hamiltonian takes the form [19]:

$$H_W^{(\Delta S = 1)} = \frac{G_F}{\sqrt{2}} \cos\theta_c \sin\theta_c \, [\, \bar{d}_a \gamma^\mu (1+\gamma_5) u^a \bar{u}_b \gamma_\mu (1+\gamma_5) s^b \qquad (6.1.2)$$

$$- \, \bar{d}_a \gamma^\mu (1+\gamma_5) c^a \bar{c}_b \gamma_\mu (1+\gamma_5) s^b \,]$$

This operator has the required $\Delta S = 1$ structure. Because we will only compute the ratio of matrix elements, from now on we will ignore the overall factor in (6.1.2). Also we have made the assumption that there are only two generations of quarks. We shall make some more comments about this shortly. We note that ambiguities could arise because the two currents that constitute (6.1.2) do not

commute. If we were to commute these two operators, then we get an additional operator of the form:

$$[J_1 , J_2] = \bar{d}(1+\gamma_5)s \tag{6.1.3}$$

In fact, (6.1.2) is not the leading term in the O.P.E. but rather we could have included terms of the form:

$$\bar{d}\gamma^\mu(1+\gamma_5)[\partial_\mu s] , \qquad [\partial_\mu \bar{d}]\gamma^\mu(1+\gamma_5)s \tag{6.1.4}$$

The actual combination of these operators, and their coefficients will not concern us. Using the equations of motion (we are as close to on shell as we can get) we can collapse the operators of (6.1.4) to terms like that of (6.1.3). We will ignore these terms on the grounds that the operators (6.1.3) and (6.1.4) only contribute to an offdiagonal wave function renormalization [20] and therefore do not affect the physical quantities we are calculating. To ensure that we have eliminated all unphysical offdiagonal wave function renormalizations, we take the four-fermion operator of (6.1.2) to be normal ordered. The procedure of normal ordering transfers from the continuum to the lattice formulation without any complications as was pointed out in Chap.5.

So far we have left QCD completely intact; however, when we shift to the lattice theory, we will be neglecting the high frequency modes of QCD because of the lattice cutoff. We should include these modes now by integrating them out. Because the high frequency modes are weakly coupled (asymptotic freedom), a perturbative calculation to one loop and then summing leading logarithms should perform a satisfactory job. The ingoing and outgoing legs of the operator in (6.1.2) are not in definite color states, so we do not expect (6.1.2) to be multiplicatively renormalized. Instead, consider the operators:

$$O_\pm = \bar{d}_a \Gamma^\mu u^a \, \bar{u}_b \Gamma_\mu s^b \pm \bar{d}_b \Gamma^\mu u^a \, \bar{u}_a \Gamma_\mu s^b - (u \leftrightarrow c) \tag{6.1.5a}$$

$$= \bar{d}_a \Gamma^\mu u^a \, \bar{u}_b \Gamma_\mu s^b \pm \bar{d}_a \Gamma^\mu s^a \, \bar{u}_b \Gamma_\mu u^b - (u \leftrightarrow c) \tag{6.1.5b}$$

The second step is achieved by a Fierz rearrangement. Now O_+ transforms as a **6** under color SU(3) and O_- as a $\bar{3}$. The anomalous dimensions of these operators have been calculated previously [2][19] to be:

$$\gamma_+ = \frac{1}{4\pi^2} g^2 \tag{6.1.6a}$$

$$\gamma_- = -\frac{1}{2\pi^2} g^2 \tag{6.1.6b}$$

Now we can run the effective weak Hamiltonian down to the scale of the c (and s for this calculation) quark mass. The result is:

$$H_W = h_+(\mu) O_+ + h_-(\mu) O_- \tag{6.1.7a}$$

$$h_+(\mu) = \left[\frac{\alpha_s(\mu)}{\alpha_s(m_W)} \right]^{-6/25} \tag{6.1.7b}$$

$$h_-(\mu) = \left[\frac{\alpha_s(\mu)}{\alpha_s(m_W)} \right]^{12/25} \tag{6.1.7c}$$

The matching conditions being $h_\pm(M_W) = 1$. We immediately notice that $h_- > h_+$ and so O_- is probably enhanced over O_+. μ which will equal the inverse lattice spacing, should be chosen to satisfy $\Lambda_{QCD} \ll \mu \ll M_W$. $\mu \approx m_c$ would be appropriate. At this juncture it is instructive to consider the isospin violating properties of these operators. O_+ consists of both $\Delta I_N = 1/2$ and $\Delta I_N = 3/2$ pieces. O_- is pure $\Delta I_N = 1/2$ so we might suspect that the perturbative enhancement of O_- is the origin of the effect we wish to explain; however, the above mechanism is too feeble. Since the enhancement we see here is so small, we shall

not consider it further. For our calculation, keep in mind that both of these operators contain both $\Delta I_W = 1$ and $\Delta I_W = 2$ pieces.

The form of the Hamiltonian quoted in (6.1.2) assumes that there are only four quark flavors. If we had instead chosen to work with six or more quarks then (6.1.2) would have to be modified appropriately. By the time that we had integrated down to the scale of the c quark we would have, in addition to the operators $O_\pm$, operators such as:

$$\sum_q \bar{s}\gamma^\mu(1+\gamma_5)d\ \bar{q}\gamma_\mu(1-\gamma_5)q \tag{6.1.8a}$$

$$\sum_q \bar{s}\gamma^\mu(1+\gamma_5)\lambda_A d\ \bar{q}\gamma_\mu(1-\gamma_5)\lambda_A q \tag{6.1.8b}$$

$$[\ m_s \bar{s}\ \sigma_{\mu\nu}(1+\gamma_5)\lambda_A\ d \pm m_d \bar{s}\ \sigma_{\mu\nu}(1-\gamma_5)\lambda_A\ d\ ]G_A{}^{\mu\nu} \tag{6.1.8c}$$

These operators have been considered by previous authors [21][22], but no suggestion of any real gain over the four quark model was revealed. For our calculation we have kept the c quark in preference to integrating it out, so we still have the **GIM** mechanism. To remove the c quark would require us to split it in mass from the s quark, which as we have already pointed out, is very difficult in our context. Hence, the Penguin operators are included dynamically in our calculation and therefore their contributions will appear as the result of inexact **GIM** cancellations.

Using the generation representation for the fermions the four operators are:

$$O_1{}^{(1)} = \bar{\psi}_1\gamma^\mu(1+\gamma_5)\tau_-\psi_1\ \bar{\psi}_1\gamma_\mu(1+\gamma_5)\tau_+\psi_2 \tag{6.1.9a}$$

$$O_1{}^{(2)} = \bar{\psi}_1\gamma^\mu(1+\gamma_5)\tau_-\psi_2\ \bar{\psi}_2\gamma_\mu(1+\gamma_5)\tau_+\psi_2 \tag{6.1.9b}$$

$$O_2{}^{(1)} = \bar{\psi}_1\gamma^\mu(1+\gamma_5)(1-\tau_3)\psi_2\ \bar{\psi}_1\gamma_\mu(1+\gamma_5)(1+\tau_3)\psi_1 \tag{6.1.9c}$$

$$O_2^{(2)} = \overline{\psi}_1\gamma^\mu(1+\gamma_5)(1-\tau_3)\psi_2\,\overline{\psi}_2\gamma_\mu(1+\gamma_5)(1+\tau_3)\psi_2 \qquad (6.1.9d)$$

Eventually, we will have to break these operators into their constituent pieces and construct the lattice operators individually. We will postpone this step until the next chapter; however, we can describe how the construction will be carried out in general.

6.3. The Lattice Hamiltonian

The methods used for this construction are identical to those used to construct the bilinears tabulated in Appendix A. Given those results we may easily obtain the four-fermion operators as follows. Note that we use the forms of the operators that are manifestly eigenstates of parity.

$$\int d^3x\,\overline{q}\Gamma_i q \;\rightarrow\; \sum_r B_i(r) \qquad (6.2.1a)$$

$$\int d^3x\,\overline{q}\Gamma_1 q\,\overline{q}\Gamma_2 q \;\rightarrow\; \sum_r B_1(r)B_2(r) \qquad (6.2.1b)$$

It can be easily checked that that the four-fermion operator (6.2.1b) has the appropriate transformation properties under any lattice operation if the constituent bilinears (6.2.1a) have the appropriate properties. The transformation law under parity is manifest by the construction of B_1 and B_2 in section (5.1). Normal ordering is taken to be implicit in (6.2.1).

There is another minor complication that we must consider. With the color indices included, these operators are only globally gauge invariant. When we modify the operators to enforce local SU(3) color invariance there will be an ambiguity for operators that span more than on link, e.g.,

$$\chi^\dagger(r)\chi(r+n_x+n_y) \qquad (6.2.2)$$

could generalize to either of:

$$\chi^{\dagger}(r)\,U(r,n_x)\,U(r+n_x,n_y)\,\chi(r+n_x+n_y) \tag{6.2.3a}$$

$$\chi^{\dagger}(r)\,U(r,n_y)\,U(r+n_y,n_x)\,\chi(r+n_x+n_y) \tag{6.2.3b}$$

This problem is easy to fix; we just weight each possibility with $(n!)^{-1}$ where n is the number of links which are spanned. There is no real principle invoked here; rather, *"If in doubt, Symmetrize"*. Obviously, this causes a terrible proliferation in the number of operators which must be considered.

There is a final delicate problem that we must worry about. We have to be able to fix the relative normalizations between the constituent pieces of the lattice weak Hamiltonian. There are no points of physics involved, rather, one must just be careful.

7 : The Matrix Elements

Finally, we come to the actual calculation of the matrix elements we are interested in. Before we plunge into the explicit construction, and evaluation, of the strong coupling graphs we will take a moment to look at the symmetries within the matrix elements we are computing. There are very many graphs to deal with and therefore any simplification will be a considerable gain, even if only in computer time. The following arguments are independent of the explicit forms of the wave functions and operators.

7.1. Symmetries

The first point to notice is that by the Wigner–Eckart theorem:

$$\begin{aligned} \langle\, \pi^+\pi^0 \,|H_{3/2}|\, K^+ \,\rangle \;&=\; \langle I_N{=}2, I_{N3}{=}1 \,|H_{3/2}|\, I_N{=}\tfrac{1}{2}, I_{N3}{=}\tfrac{1}{2} \,\rangle \\ &=\; \left(\frac{3}{2}\right)^{1/2} \langle I_N{=}2, I_{N3}{=}0 \,|H_{3/2}|\, I_N{=}\tfrac{1}{2}, I_{N3}{=}-\tfrac{1}{2} \,\rangle \end{aligned} \tag{7.1.1}$$

Hence, the only final state wave functions we have to consider are (2.3b) and (2.3c) for the $\Delta I_N = 3/2$ and $\Delta I_N = 1/2$ amplitudes respectively. Following the definition (5.2.3), and recognizing the minus sign, we write:

$$\pi^+\pi^- \;+\; \pi^-\pi^+ \;=\; -\left[\, \pi^1\pi^1 \;+\; \pi^2\pi^2 \,\right] \tag{7.1.2}$$

For convenience, we will now refer to the π^0 often as π^3. So up to an overall phase, the wave functions now take the form:

$$I = 2 \;\; I_3 = 0 \;:\quad \frac{1}{\sqrt{6}}\left(\, \pi^1\,\pi^1 \;+\; \pi^2\,\pi^2 \;-\; 2\pi^3\,\pi^3 \,\right) \tag{7.1.2a}$$

$$I = 0 \;\; I_3 = 0 \;:\quad \frac{1}{\sqrt{3}}\left(\, \pi^1\,\pi^1 \;+\; \pi^2\,\pi^2 \;+\; \pi^3\,\pi^3 \,\right) \tag{7.1.2b}$$

The matrix elements that we need to compute all have the form:

$$\langle \pi^i \pi^i \, | O_W | \, K^0 \rangle \tag{7.1.3}$$

where i ranges from one to three and O_W is the lattice version of any of the operators detailed in (6.1.9). We now use the known transformation properties of both the wave functions and the operators to reduce these matrix elements to a minimal set. Because the matrix elements as originally written do not couple the $\overline{D}^0$ component of the initial state to the $\pi\pi$ final state, the following manipulations will preserve this state of affairs.

The first gain we can make is to notice that the operator O_W and the initial state, now denoted by K^0 , are invariant under a lattice (iso)rotation about the z axis. Hence, we see that:

$$\langle \pi^1 \pi^1 \, | O_W | \, K^0 \rangle = \langle \pi^2 \pi^2 \, | O_W | \, K^0 \rangle \tag{7.1.4a}$$

$$\langle (\pi^3 \pi^3)_y \, | O_W | \, K^0 \rangle = \langle (\pi^3 \pi^3)_x \, | O_W | \, K^0 \rangle \tag{7.1.4b}$$

This reduces our calculation by a third. The components of the $\pi^3\pi^3$ wave function refer to the two parts of (5.4.3). Next, we have to break O_W down into its components stepwise. We write O_W so that its chiral structure is manifest to get:

$$O_W = [J^\mu + J_5{}^\mu][J_\mu + J_{5\mu}] \tag{7.1.5}$$

The J^μ , $J_5{}^\mu$ are flavor currents and have nontrivial transformations under (chiral) flavor rotations. Under parity, the $\pi\pi$ state is even and the K^0 state is odd, so only the cross terms in (7.1.5) will contribute. Now one can see why we took some pains to ensure that space reflection symmetry was manifest in our operators.

To make progress beyond this point, we must now specialize attention to specific flavor structures within the currents. From (6.1.9) the currents come in two types:

$$O_1 = \overline{\psi}\Gamma(\tau_1 - i\tau_2)\psi\,\overline{\psi}\Gamma'(\tau_1 + i\tau_2)\psi \tag{7.1.6a}$$

$$O_2 = \overline{\psi}\Gamma(1 - \tau_3)\psi\,\overline{\psi}\Gamma'(1 + \tau_3)\psi \tag{7.1.6b}$$

The ψ and Γ are generic. Now, consider a flavor rotation $\psi \to \tau_1\psi$. The $\pi^i\pi^i$ components of the pion wave function are invariant while the K^0 reverses sign. So, again only the cross terms in both (7.1.6a) and (7.1.6b) will contribute. Note that we are unable to make any use of the now broken chiral symmetries to reduce the matrix elements.

We can go even further, if we look at specific final state components and spatial components of the currents. Independently of the chiral or flavor structure of the currents we can easily show, using a rotation about the z axis, that:

$$\langle\, \pi^3\pi^3 \,|J_5{}^x J^x|\, K^0 \,\rangle = \langle\, \pi^3\pi^3 \,|J_5{}^y J^y|\, K^0 \,\rangle \tag{7.1.7a}$$

$$\langle\, \pi^3\pi^3 \,|J^x J_5{}^x|\, K^0 \,\rangle = \langle\, \pi^3\pi^3 \,|J^y J_5{}^y|\, K^0 \,\rangle \tag{7.1.7b}$$

For simplicity, we have used the continuum language. These results are independent of the form of the operators and will hold on the lattice. We can also make the following simplifications:

$$\langle\, \pi^3\pi^3 \,|J_5{}^t(\tau_1) J^t(\tau_2)|\, K^0 \,\rangle = -\langle\, \pi^3\pi^3 \,|J_5{}^t(\tau_2) J^t(\tau_1)|\, K^0 \,\rangle \tag{7.1.8a}$$

$$\langle\, \pi^3\pi^3 \,|J^t(\tau_1) J_5{}^t(\tau_2)|\, K^0 \,\rangle = -\langle\, \pi^3\pi^3 \,|J^t(\tau_2) J_5{}^t(\tau_1)|\, K^0 \,\rangle \tag{7.1.8b}$$

$$\langle \pi^3\pi^3 \,|J_5{}^z(\tau_1)J^z(\tau_2)\,|K^0\rangle = -\langle \pi^3\pi^3 \,|J_5{}^z(\tau_2)J^z(\tau_1)\,|K^0\rangle \qquad (7.1.8c)$$

$$\langle \pi^3\pi^3 \,|J^z(\tau_1)J_5{}^z(\tau_2)\,|K^0\rangle = -\langle \pi^3\pi^3 \,|J^z(\tau_2)J_5{}^z(\tau_1)\,|K^0\rangle \qquad (7.1.8d)$$

It is not always convenient to implement all of these symmetries; rather, we prefer to use some of them for the actual calculation and the remainder as checks on partial results. We are now poised and ready to calculate.

7.2. A Sample Calculation

The full calculation is too extensive for us to provide all the details, so instead, we will illustrate some of the features by examining select operators in detail. One of the operators is taken from $O_1{}^{(1)}$ and the other from $O_1{}^{(2)}$. The balance of the calculation is identical in substance.

7.2.1. Zeroth Order

The matrix element that we evaluate is, with $\psi_0{}^{(1)}$ representing the Kaon wave function (5.3.2) and $\psi_0{}^{(2)}$ the appropriate two pion state:

$$\langle \psi_0{}^{(2)}\,|H_W\,|\psi_0{}^{(1)}\rangle \qquad (7.2.1)$$

The operators that we choose as examples are:

$$A_W = \overline{\psi}_1\gamma^t\gamma_5\tau_2\psi_1\,\overline{\psi}_1\gamma^t\tau_1\psi_2 \qquad (7.2.2a)$$

$$B_W = \overline{\psi}_1\gamma^t\gamma_5\tau_2\psi_2\,\overline{\psi}_2\gamma^t\tau_1\psi_2 \qquad (7.2.2b)$$

Explicit forms for A_W and B_W can be read off Table B.1. Notice that B_W is the "**GIM** conjugate" operator of A_W and will appear with a relative minus sign.

There is an important simplification at this level as all of the graphs derived from the operators $O_1^{(2)}$ and $O_2^{(2)}$ obviously vanish. This is an interesting observation because these are all graphs that would become the "Penguins" if we were to integrate out the c quark. Hence, we only have to evaluate A_W . Allowing for the various configurations of the SU(3) matrices, there are two nonvanishing graphs corresponding to the operator A_W where one of these is a mirror reflection of the other. The unique distinct graph is presented in Fig.5(a). This graph evaluates simply to "3" , the answer being independent of all other parameters such as quark masses, etc.

When we complete the calculation we discover a remarkable, and certainly unexpected, result; the entire contribution for zeroth order vanishes identically. In essence, the reason for this cancellation is luck. If one expands the expressions for the operators J^tJ^t and J^zJ^z , the cancellation can be seen to be an accident that will not persist at second order. A similar phenomenon occurs for the J^xJ^x and J^yJ^y constituent operators of O_2 .

7.2.2. First Order

The contributions to the matrix element are:

$$\left\langle \psi_0^{(2)} \right| V \frac{Q}{(E_0^{(2)} - H_0)} H_W \left| \psi_0^{(1)} \right\rangle + \left\langle \psi_0^{(2)} \right| H_W \frac{Q}{(E_0^{(1)} - H_0)} V \left| \psi_0^{(1)} \right\rangle \qquad (7.2.3)$$

These matrix elements will vanish if V represents the kinetic Hamiltonian for the fermions. However, if V is taken to be the magnetic part of the gauge fields, then this matrix element need not vanish. Fig.5(b) depicts the two possible nonvanishing graphs (they are time orderings) that one derives from the zeroth order configuration. The first evaluates to $-1/12$; the second graph will not appear due to the vanishing of the energy denominator.

For exactly the same reasons as the previous order, when all diagrams are summed, these contributions will cancel. Hence, it is left to second order to pick up a nonvanishing matrix element.

7.2.3. Second Order

These matrix elements also go as g^{-4} if the perturbing Hamiltonian is taken to be the fermion kinetic Hamiltonian. The matrix element takes the form:

$$\left\langle \psi_0^{(2)} \right| V \frac{Q}{(E_0^{(2)} - H_0)} V \frac{Q}{(E_0^{(2)} - H_0)} H_W \left| \psi_0^{(1)} \right\rangle + \text{CYCLIC} \tag{7.2.4}$$

At this stage, we first begin to see disconnected graphs. We will divide our discussion into the disconnected and then the connected pieces.

7.2.3.1. Disconnected Amplitudes

Because the zeroth order matrix elements vanished, there will be no graphs that are derived from vacuum bubbles. The only contribution that we will get comes from the graphs in which the weak Hamiltonian annihilates the Kaon and the strong interaction creates the pair of pions. With the requirement that H_W be normal ordered, these graphs are trivially zero; however, it is interesting to note that in any other ordering scheme, the graphs would have evaluated to:

$$\begin{aligned} \left\langle \pi^3\pi^3 \right| O_1 \left| K^0 \right\rangle \approx \Big\{ & \left[\tfrac{4}{3} + 60A_1 + 2m_u\right]^{-1} \left[\tfrac{4}{3} + 68A_1 + 2m_u\right]^{-1} \\ & - \left[\tfrac{4}{3} + 60A_1 + 2m_u\right]^{-1} \left[\tfrac{8}{3} + 128A_1 + 4m_u\right]^{-1} \\ & - \left[\tfrac{4}{3} + 68A_1 + 2m_u\right]^{-1} \left[\tfrac{8}{3} + 128A_1 + 4m_u\right]^{-1} \Big\} \end{aligned} \tag{7.2.5}$$

Expanding, we observe that (7.2.5) vanishes identically due to a cancellation among the energy denominators. It is reassuring that the disconnected graphs vanish because this amplitude has an overall factor of the volume of the lattice.

7.2.3.2. Connected Amplitudes

With the disconnected graphs behind us we now attack the connected parts and proceed to the final result.

Within this portion of the calculation there are two contributions that we wish to isolate; the "Penguin" graphs, and the remainder. We might think that it would be straightforward to construct all of the "Penguins" because the operators $O_i^{(2)}$ are purely "Penguin" contributions. From these we could then work back to construct those graphs which are derived from u–quark loops. Unfortunately, this approach fails. Heuristically, the reason can be illustrated with the following example. Fig.6(b). presents a graph derived from B_W and Fig.6(a). what we would expect the corresponding u–quark loop graph to be. That Fig.6(b). is a "Penguin" is correct; the claim that Fig.6(a). only contributes to the "Penguin" graphs is not. Rather, the time orderings of this graph individually contribute both to "Penguin" *and* to non–"Penguin" amplitudes. Although these particular graphs will not appear for the same reason that zeroth and first order amplitudes vanish, the problem they demonstrate is generic. The important point is that there is not a one to one correspondence between Strong Coupling graphs and the Feynman diagrams of weak coupling perturbation theory. As a result, it is extremely difficult to isolate the purely "Penguin" parts of the operators. If the c–quark loops as indicative of the magnitudes of the u–quark loops, then the "Penguin" graphs are irrelevant.

The remaining calculation entails the construction of just over 2000 graphs, which swells to about 12000 graphs when the time orderings are counted. The final computations produce roughly 6300 nonzero amplitudes. Because this calculation has been fully automated, we will only present the results.

It is not possible to choose *a priori* a particular value for A_1 therefore we have plotted the results against this parameter of our calculation. The graph is presented in Fig.7. Below, we present the expectation values of the operators using three representative values for the coefficient of the irrelevant operators; $A_1 = 0.02$, 0.10, and 1.00. The reader should recall that A_1 is bounded below by $1/84$. The common u,d quark mass is taken to be zero. A pesky overall factor of i has been dropped to give the quoted results.

$\langle I_W = I_N = 0 \mid O_W \mid I_W = 1 \rangle$

O_W	$A_1 = 0.02$	$A_1 = 0.1$	$A_1 = 1$
$O_1^{(1)}$	10.9566	2.1495	0.1690
$O_1^{(2)}$	−0.0012	−0.0003	−0.0000
$O_2^{(1)}$	9.0137	2.1200	0.1685
$O_2^{(2)}$	−0.0088	−0.0003	−0.0000
O_+	19.9803	4.2701	0.3376
O_-	1.9353	0.0295	0.0005

$\langle I_W = I_N = 2 \mid O_W \mid I_W = 1 \rangle$

O_W	$A_1 = 0.02$	$A_1 = 0.1$	$A_1 = 1$
$O_1^{(1)}$	6.2159	0.0553	−0.0483
$O_1^{(2)}$	−0.0195	−0.0007	−0.0000
$O_2^{(1)}$	4.9785	0.0464	−0.0485
$O_2^{(2)}$	0.0026	−0.0005	−0.0000
O_+	11.2112	0.1028	−0.0968
O_-	1.2595	0.0091	0.0002

7.3. Discussion

The most outstanding feature of these results is the very strong suppression of the operators $O_i^{(2)}$ for both decay channels. The origin of this result appears to be a cancellation among the contributing graphs; the values of individual graphs from any of the four constituent operators tend to be of the same order of magnitude although some will diverge as $A_1 \to 0$. Contrary to what one might expect this suppression is not entirely due to the c-quark mass; the phenomenon persists even for $m_s^{(0)} = 0$ and for $A_2 \approx A_1$.

Another feature that sets these results apart from what we might expect in a continuum calculation is the nonvanishing matrix element of O_- that we observe in the $I = 2$ final state channel. In the continuum we would expect that this matrix element would vanish due to the now near exact "nuclear" isospin symmetry. Presumably, if we were able to extend these calculations to the

continuum, then we would be able to see the restoration of "nuclear" isospin symmetry. The size of this matrix element can serve to give us a vague indication of how close we are to the continuum limit.

Because there is no "nuclear" isospin, the best way to search for a $\Delta I_N = 1/2$ effect is to recall from Chap.1. that this rule is equivalent to saying that the $I = 0$ final state is greatly preferred. Looking at our results, it turns out that in the $I = 2$ channel the amplitude vanishes within $0.10 < A_1 < 0.12$. The amplitude for decay to the $I = 0$ state never vanishes. The exact location of this zero does not concern us, e.g., it would be shifted slightly if we included the effect of perturbative QCD as discussed in Chap.6. but this is not important for our qualitative discussion. In the vicinity of this zero, the $I = 0$ final state amplitude is strongly enhanced relative to the $I = 2$ amplitude. Elsewhere, there is a always a mild enhancement of a factor of two to four.

Decomposing the operators into representations of "weak" isospin may shed some light on what is happening. The linear combination of operators that mediate the decay to the isospin singlet final state have to be $I_W = 1$ whereas the other operators are a combination of $I_W = 1$ and 2. This statement of the enhancement that we are seeing is similar, but not entirely equivalent, to the traditional explanation of the $\Delta I_N = 1/2$ rule as "Octet Dominance".

Is this enhancement the $\Delta I_N = 1/2$ rule, or is it just a quirk caused by the irrelevant operators? In the region $0.06 < A_1 < 0.20$ the contribution of these operators is similar in magnitude to other terms in the energy denominators. At 0.02 the absence of baryon–antibaryon pairs will hurt, and at 1.00 the irrelevant operators dominate the result which is unsatisfactory. This notion of prescribing values for the coefficients of the irrelevant operators is due to Banks. *et al.* [8]. The range over which we would get a ratio of greater than ten is $0.06 < A_1 < 0.20$

which we think is a very satisfactory result.

A related calculation the we could execute is to find the value of the ratio ε'/ε relevant to CP violation. A sketch of this calculation is given in Appendix D and the results are presented in Fig.8. The interesting point to notice is that this ratio also vanishes somewhere in the interval $0.10 < A_1 < 0.12$. That this result agrees qualitatively with the experimental observations in the range $0.10 < A_1 < 0.12$, and with the qualitative features of the decay amplitudes, is very encouraging.

The downside of this calculation has been that we have had to interpret the results in the strong coupling limit. Because of the vanishing of the first two orders of perturbation theory we were unable to use a padé type extrapolation to the weak coupling regime. The interpretation is further confused because of the strong dependence of the computed results on the parameter A_1. To what degree these complaints invalidate the results is unknown. Given that we do see a $\Delta I_N = 1/2$ enhancement, we suspect that the details of how we approach the continuum limit may not be that important. This would be the case if it were the strongly coupled modes of QCD that are primarily responsible for the $\Delta I_N = 1/2$ rule and the very small value of ε'/ε.

8 : Conclusion

8.1. The $\Delta I_N = 1/2$ Rule

The final conclusion is very straightforward and direct. We *do* see evidence for the $\Delta I_N = 1/2$ Rule in the Strong Coupling Limit of the Hamiltonian Lattice Theory with Kogut–Susskind fermions. In the interval $0.10 < A_1 < 0.12$ the matrix element corresponding to $\Delta I_N = 3/2$ vanishes. As corroborating evidence, we find that in the same interval the ratio ε'/ε also vanishes. This is much more than we need to explain the experimental result; indeed, there is a range of $0.06 < A_1 < 0.20$ for which the ratio of the decay amplitudes is greater than ten.

This calculation also produced a number of surprises.

[1] The result that we found most surprising was the vanishing of the weak matrix elements for the first two orders of strong coupling perturbation theory. One expects QCD to modify matrix elements, but not to make them vanish. This result appears to be a quirk of Kogut–Susskind fermions therefore it would be interesting to see if this kind of behavior should exist for other weak processes that are calculated by the methods used here.

[2] The dominance of the O_+ operators which is the exact opposite of what the folklore from weak coupling perturbation theory expects.

[3] The suppression of the c–quark loops which appears to be the consequence of some kind of cancellation among the graphs; rather than the signature of a large c mass.

8.2. Computer Algebra : A Few Comments

Irrespective of the results that we obtained above, we think that it is worth making a few comments about the use of computer algebra as applied to this kind of problem.

The primary advantage of this technique is that you know exactly what physics has been included in a calculation, and what has been left out. Any kind of averaging was done explicitly before the calculations were undertaken. There are also technical advantages; e.g, there is never a problem with roundoff error although if one is not using arbitrary precision arithmetic, integer overflow can be a problem.

The major disadvantage of these methods is that the final answer often turns out to be a huge mess of terms which provide very little insight. In this situation, which is the one that pertains here, one has little choice but to numerically evaluate the result. This is not as bad as it might appear though, for evaluating the result is easy to do, and if desired, very fine resolution graphs can be produced.

As a final comment, we believe that computer algebra approaches have a great application in physics, especially when used in conjunction with other methods.

References

[1] C.G. Wohl *et al.*, Rev. Mod. Phys. **56(2)** (1984)

[2] M.K. Gaillard and B.W. Lee, Phys. Rev. Lett. **33** (1974) 108.

G. Altarelli and L. Maiani, Phys. Lett. **52B** (1974) 351.

[3] C. Bernard *et al.*, Phys. Rev. Lett. **55** (1985) 2770.

C. Bernard, UCLA–84–TEP–03.

C. Bernard *et al.*, UCLA/84/TEP/14 (1984)

[4] O. Martin and A. Patel, UCSD–10P10–252 and ILL–TH–85–64 (1985).

[5] J. F. Donoghue, E. Golowich, and B. Holstien, Phys. Rep. **131(5&6)** (1986)

L. Chau, Phys. Rep. **95(1)** (1983)

[6] K.G. Wilson, Phys. Rev. **D10** (1974) 2445.

[7] J. Kogut, D.K. Sinclair, and L. Susskind, Nucl. Phys. **B114** (1976) 199.

[8] T. Banks *et al.*, Phys. Rev. **D15** (1977) 1111.

[9] J.B. Kogut *et al.*, Phys. Rev. **D23** (1981) 2945.

[10] L. Susskind, Phys. Rev. **D16** (1977) 3031.

[11] T. Banks, SLAC–PUB–3876 (1986).

[12] A. Messiah, *Quantum Mechanics Vol. II*, North Holland 1962.

[13] R. Balin, J.M. Drouffe, and C. Itzkson, Phys. Rev. **D11** (1975) 2104.

[14] J.B. Kogut, Rev. Mod. Phys. **55(3)** (1983) 775.

[15] A.C. Irving, C.J. Hamer, Nucl. Phys. **B235** (1984) 358.

A.C. Irving, C.J. Hamer, Nucl. Phys. **B240** (1984) 362.

C.J. Hamer, A.C. Irving, Nucl. Phys. **B230** (1984) 336.

A.C. Irving, C.J. Hamer, Nucl. Phys. **B230** (1984) 361.

[16] J.B. Kogut, R.B. Pearson, J. Shigemitsu, Phys. Lett. **98B** (1981) 63.

[17] J.D. Bjorken and S.D. Drell, *Relativistic Quantum Fields*, McGraw–Hill 1965.

[18] D.R.T. Jones, *et al.*, Nucl. Phys. **B158** (1979) 102.

A. Carroll, J.B. Kogut, Phys. Rev. **D19** (1979) 2429.

[19] H. Georgi, *Weak Interactions and Modern Particle Theory*, Benjamin 1984.

[20] G. Feinberg, P. Kabir, S. Weinberg, Phys. Rev. Lett. **3** (1959) 527

[21] C.T. Hill and G.G. Ross, Nucl. Phys. **B171** (1980) 141.

[22] F.J. Gillman and M.B. Wise, Phys. Rev. **D20** (1979) 2392

Appendix A : Kogut–Susskind Fermions

Table A.1 : Symmetries of the Hamiltonian

Lattice Formulation	Continuum Equivalent
$\chi(r) \rightarrow \chi^{\dagger}(r)$	G–Parity
$\chi(r) \rightarrow (-1)^{y}\chi(r+n_x)$ $\chi(r) \rightarrow (-1)^{z}\chi(r+n_y)$ $\chi(r) \rightarrow (-1)^{x}\chi(r+n_z)$	$\psi \rightarrow -i\gamma_5\tau_1\psi$ $\psi \rightarrow i\gamma_5\tau_2\psi$ $\psi \rightarrow i\gamma_5\tau_3\psi$
$\chi(r) \rightarrow (-1)^{x+z}\chi(r+n_y+n_z)$ $\chi(r) \rightarrow (-1)^{y+x}\chi(r+n_z+n_x)$ $\chi(r) \rightarrow (-1)^{z+y}\chi(r+n_x+n_y)$	$\psi \rightarrow -i\tau_1\psi$ $\psi \rightarrow i\tau_2\psi$ $\psi \rightarrow i\tau_3\psi$
$\chi(r) \rightarrow (-1)^{x+y+z}\chi(r+n_x+n_y+n_z)$	$\psi \rightarrow \gamma_5\psi$
$\chi(r) \rightarrow \chi(r+2n_i)$	Translations
$\chi(r) \rightarrow D(x,y)D(y,z)D(z,x)\chi'(r')$	(Iso)Rotations of $\pi/2$
$\chi(r) \rightarrow \chi'(-r)$	Parity, Reflections
$\chi(r) \rightarrow \chi(Rr)$	Rotations of π
$x \rightarrow y \rightarrow z$ $-\tau_1 \rightarrow \tau_2 \rightarrow \tau_3$	Cyclic Permutations

SU(4) Discrete Flavor Symmetry

With two generations of fermions, the flavor symmetry becomes $SU(2)_g \otimes SU(2)_d$, where the $SU(2)_g$ is a continuous symmetry that transforms fields between generations. The other group is the discrete subgroup of SU(2) that acts within each Kogut–Susskind field simultaneously. We have ignored the complications that chirality introduces to the group structure.

Within this symmetry group, we can find a discrete subgroup of the SU(4) flavor symmetry. The basic elements of this symmetry are related to the SU(4) generators by:

$$i\,T \;=\; e^{i\frac{\pi}{2}T} \tag{A.1}$$

The transformations are:

$$T^0{}_i \;=\; \begin{bmatrix} \tau_i & 0 \\ 0 & \tau_i \end{bmatrix} \qquad T^3{}_i \;=\; \begin{bmatrix} \tau_i & 0 \\ 0 & -\tau_i \end{bmatrix}$$

$$T^1{}_i \;=\; \begin{bmatrix} 0 & \tau_i \\ \tau_i & 0 \end{bmatrix} \qquad T^2{}_i \;=\; \begin{bmatrix} 0 & -i\tau_i \\ i\tau_i & 0 \end{bmatrix}$$

$$T^1 \;=\; \begin{bmatrix} 0 & I \\ I & 0 \end{bmatrix} \qquad T^2 \;=\; \begin{bmatrix} 0 & -iI \\ iI & 0 \end{bmatrix}$$

$$T^3 \;=\; \begin{bmatrix} I & 0 \\ 0 & -I \end{bmatrix}$$

Table A.2 : Bilinears; Flavor Singlets

Continuum	Lattice Bilinear	η_P	η_C
$\overline{\psi}\psi$	$\chi^\dagger(r)\chi(r)(-1)^{x+y+z}$	0	0
$\overline{\psi}\gamma^t\psi$	$\chi^\dagger(r)\chi(r)$	0	0
$\overline{\psi}\gamma^x\psi$	$-i(-1)^z\chi^\dagger(r)\chi(r+n_x)$	−1	−1
$\overline{\psi}\gamma^y\psi$	$-i(-1)^x\chi^\dagger(r)\chi(r+n_y)$	−1	−1
$\overline{\psi}\gamma^z\psi$	$-i(-1)^y\chi^\dagger(r)\chi(r+n_z)$	−1	−1
$\overline{\psi}\gamma_5\psi$	$\sum_{abc}\eta_{abc}\chi^\dagger(r)\chi(r+an_x+bn_y+cn_z)$ $\eta_{+++}=\eta_{+--}=\eta_{-+-}=\eta_{--+}=1$	−1	−1
$\overline{\psi}\gamma^t\gamma_5\psi$	$\sum_{abc}\eta_{abc}(-1)^{x+y+z}\chi^\dagger(r)\chi(r+an_x+bn_y+cn_z)$ $\eta_{+++}=\eta_{+--}=\eta_{-+-}=\eta_{--+}=1$	−1	+1
$\overline{\psi}\gamma^x\gamma_5\psi$	$-i(-1)^{x+y}\chi^\dagger(r)[\chi(r+n_y+n_z)-\chi(r+n_y-n_z)]$	+1	−1
$\overline{\psi}\gamma^y\gamma_5\psi$	$-i(-1)^{y+z}\chi^\dagger(r)[\chi(r+n_z+n_x)-\chi(r+n_z-n_x)]$	+1	−1
$\overline{\psi}\gamma^z\gamma_5\psi$	$-i(-1)^{x+z}\chi^\dagger(r)[\chi(r+n_x+n_y)-\chi(r+n_x-n_y)]$	+1	−1

The phase convention that we follow for η_C is that if the bilinear is hermitian; then $\eta_C = 1$ if there is no overall factor of i, and $\eta_C = -1$ if there is the imaginary factor.

Table A.3 : Bilinears; Vector Flavor Triplets

Continuum	Lattice Bilinear	η_P	η_C
$\overline{\psi}\gamma^t\tau_1\psi$	$i\,(-1)^{z+x}\,\chi^\dagger(r)\,[\,\chi(r+n_y+n_z)-\chi(r+n_y-n_z)\,]$	$+1$	-1
$\overline{\psi}\gamma^x\tau_1\psi$	$-\sum_{abc}\eta_{abc}\,(-1)^x\chi^\dagger(r)\chi(r+an_x+bn_y+c\,n_z)$	-1	$+1$
	$\eta_{+++}=\eta_{+--}=\eta_{-+-}=\eta_{--+}=1$		
$\overline{\psi}\gamma^y\tau_1\psi$	$-(-1)^z\chi^\dagger(r)\chi(r+n_z)$	-1	$+1$
$\overline{\psi}\gamma^z\tau_1\psi$	$(-1)^{x+y+z}\,\chi^\dagger(r)\,\chi(r+n_y)$	-1	$+1$
$\overline{\psi}\gamma^t\tau_2\psi$	$-i\,(-1)^{x+y}\,\chi^\dagger(r)\,[\,\chi(r+n_z+n_x)-\chi(r+n_z-n_x)\,]$	$+1$	-1
$\overline{\psi}\gamma^x\tau_2\psi$	$-(-1)^{x+y+z}\,\chi^\dagger(r)\,\chi(r+n_z)$	-1	$+1$
$\overline{\psi}\gamma^y\tau_2\psi$	$\sum_{abc}\eta_{abc}\,(-1)^y\,\chi^\dagger(r)\chi(r+an_x+bn_y+c\,n_z)$	-1	$+1$
	$\eta_{+++}=\eta_{+--}=\eta_{-+-}=\eta_{--+}=1$		
$\overline{\psi}\gamma^z\tau_2\psi$	$(-1)^x\chi^\dagger(r)\chi(r+n_x)$	-1	$+1$
$\overline{\psi}\gamma^t\tau_3\psi$	$-i\,(-1)^{y+z}\,\chi^\dagger(r)\,[\,\chi(r+n_x+n_y)-\chi(r+n_x-n_y)\,]$	$+1$	-1
$\overline{\psi}\gamma^x\tau_3\psi$	$(-1)^y\,\chi^\dagger(r)\chi(r+n_y)$	-1	$+1$
$\overline{\psi}\gamma^y\tau_3\psi$	$-(-1)^{x+y+z}\,\chi^\dagger(r)\,\chi(r+n_x)$	-1	1
$\overline{\psi}\gamma^z\tau_3\psi$	$\sum_{abc}\eta_{abc}\,(-1)^z\chi^\dagger(r)\chi(r+an_x+bn_y+c\,n_z)$	-1	$+1$
	$\eta_{+++}=\eta_{+--}=\eta_{-+-}=\eta_{--+}=1$		

Table A.4 : Bilinears; Pseudoscalar and Axial Vector Flavor Triplets

Continuum	Lattice Bilinear	η_P	η_C
$\overline{\psi}\gamma_5\tau_3\psi$	$i\,(-1)^{y+z}\,\chi^\dagger(r)\,\chi(r+n_z)$	-1	-1
$\overline{\psi}\gamma^t\gamma_5\tau_1\psi$	$i\,(-1)^{y}\,\chi^\dagger(r)\chi(r+n_x)$	-1	-1
$\overline{\psi}\gamma^x\gamma_5\tau_1\psi$	$-(-1)^{y+z}\chi^\dagger(r)\chi(r)$	0	0
$\overline{\psi}\gamma^y\gamma_5\tau_1\psi$	$-(-1)^{y+x}\chi^\dagger(r)\,[\,\chi(r+n_{y+}n_x) - \chi(r+n_y-n_x)\,]$	$+1$	$+1$
$\overline{\psi}\gamma^z\gamma_5\tau_1\psi$	$\chi^\dagger(r)\,[\,\chi(r+n_z+n_x) - \chi(r+n_z-n_x)\,]$	$+1$	$+1$
$\overline{\psi}\gamma^t\gamma_5\tau_2\psi$	$-i\,(-1)^{z}\chi^\dagger(r)\chi(r+n_y)$	-1	-1
$\overline{\psi}\gamma^x\gamma_5\tau_2\psi$	$-\chi^\dagger(r)\,[\,\chi(r+n_x+n_y) - \chi(r+n_x-n_y)\,]$	$+1$	$+1$
$\overline{\psi}\gamma^y\gamma_5\tau_2\psi$	$(-1)^{z+x}\chi^\dagger(r)\chi(r)$	0	0
$\overline{\psi}\gamma^z\gamma_5\tau_2\psi$	$(-1)^{z+y}\,\chi^\dagger(r)\,[\,\chi(r+n_z+n_y) - \chi(r+n_z-n_y)\,]$	$+1$	$+1$
$\overline{\psi}\gamma^t\gamma_5\tau_3\psi$	$-i\,(-1)^{x}\chi^\dagger(r)\chi(r+n_z)$	-1	-1
$\overline{\psi}\gamma^x\gamma_5\tau_3\psi$	$(-1)^{x+z}\,\chi^\dagger(r)\,[\,\chi(r+n_x+n_z) - \chi(r+n_x-n_z)\,]$	$+1$	$+1$
$\overline{\psi}\gamma^y\gamma_5\tau_3\psi$	$-\chi^\dagger(r)\,[\,\chi(r+n_y+n_z) - \chi(r+n_y-n_z)\,]$	$+1$	$+1$
$\overline{\psi}\gamma^z\gamma_5\tau_3\psi$	$(-1)^{x+y}\chi^\dagger(r)\chi(r)$	0	0

Looking back over the tables just presented, a word of caution is in order.

Beware of the minus sign associated with the flavor generator τ_1 .

Appendix B : Four-Fermion Operators

In the following two tables we detail, in the continuum language, all of the four-fermion operators that we need for this calculation. They are divided into two groups as constituents of O_1 and O_2 defined in (6.1.10). For convenience, these definitions have been repeated below.

$$O_1^{(1)} = \overline{\psi}_1\gamma^\mu(1+\gamma_5)(\tau_1-i\tau_2)\psi_1\,\overline{\psi}_1\gamma_\mu(1+\gamma_5)(\tau_1+i\tau_2)\psi_2 \tag{B.1a}$$

$$O_1^{(2)} = \overline{\psi}_1\gamma^\mu(1+\gamma_5)(\tau_1-i\tau_2)\psi_2\,\overline{\psi}_2\gamma_\mu(1+\gamma_5)(\tau_1+i\tau_2)\psi_2 \tag{B.1b}$$

$$O_2^{(1)} = \overline{\psi}_1\gamma^\mu(1+\gamma_5)(1-\tau_3)\psi_2\,\overline{\psi}_1\gamma_\mu(1+\gamma_5)(1+\tau_3)\psi_1 \tag{B.1c}$$

$$O_2^{(2)} = \overline{\psi}_1\gamma^\mu(1+\gamma_5)(1-\tau_3)\psi_2\,\overline{\psi}_2\gamma_\mu(1+\gamma_5)(1+\tau_3)\psi_2 \tag{B.1d}$$

In total, there are 64 operators that we must construct and then take the expectations values of. Account has not been taken of a few minor symmetries which would reduce the number of operators needed by a small number. Operators which are **GIM** conjugates are placed in the same row. These operators always have an additional minus sign associated with them.

Table B.1 : Operators for O_1

$O_1^{(1)}$	$O_1^{(2)}$	Phase
$\overline{\psi}_1\gamma^t\tau_1\psi_1\overline{\psi}_1\gamma^t\gamma_5\tau_2\psi_2$	$\overline{\psi}_1\gamma^t\tau_1\psi_2\overline{\psi}_2\gamma^t\gamma_5\tau_2\psi_2$	$+i$
$\overline{\psi}_1\gamma^t\tau_2\psi_1\overline{\psi}_1\gamma^t\gamma_5\tau_1\psi_2$	$\overline{\psi}_1\gamma^t\tau_2\psi_2\overline{\psi}_2\gamma^t\gamma_5\tau_1\psi_2$	$-i$
$\overline{\psi}_1\gamma^t\gamma_5\tau_1\psi_1\overline{\psi}_1\gamma^t\tau_2\psi_2$	$\overline{\psi}_1\gamma^t\gamma_5\tau_1\psi_2\overline{\psi}_2\gamma^t\tau_2\psi_2$	$+i$
$\overline{\psi}_1\gamma^t\gamma_5\tau_2\psi_1\overline{\psi}_1\gamma^t\tau_1\psi_2$	$\overline{\psi}_1\gamma^t\gamma_5\tau_2\psi_2\overline{\psi}_2\gamma^t\tau_1\psi_2$	$-i$
$\overline{\psi}_1\gamma^x\tau_1\psi_1\overline{\psi}_1\gamma^x\gamma_5\tau_2\psi_2$	$\overline{\psi}_1\gamma^x\tau_1\psi_2\overline{\psi}_2\gamma^x\gamma_5\tau_2\psi_2$	$+i$
$\overline{\psi}_1\gamma^x\tau_2\psi_1\overline{\psi}_1\gamma^x\gamma_5\tau_1\psi_2$	$\overline{\psi}_1\gamma^x\tau_2\psi_2\overline{\psi}_2\gamma^x\gamma_5\tau_1\psi_2$	$-i$
$\overline{\psi}_1\gamma^x\gamma_5\tau_1\psi_1\overline{\psi}_1\gamma^x\tau_2\psi_2$	$\overline{\psi}_1\gamma^x\gamma_5\tau_1\psi_2\overline{\psi}_2\gamma^x\tau_2\psi_2$	$+i$
$\overline{\psi}_1\gamma^x\gamma_5\tau_2\psi_1\overline{\psi}_1\gamma^x\tau_1\psi_2$	$\overline{\psi}_1\gamma^x\gamma_5\tau_2\psi_2\overline{\psi}_2\gamma^x\tau_1\psi_2$	$-i$
$\overline{\psi}_1\gamma^y\tau_1\psi_1\overline{\psi}_1\gamma^y\gamma_5\tau_2\psi_2$	$\overline{\psi}_1\gamma^y\tau_1\psi_2\overline{\psi}_2\gamma^y\gamma_5\tau_2\psi_2$	$+i$
$\overline{\psi}_1\gamma^y\tau_2\psi_1\overline{\psi}_1\gamma^y\gamma_5\tau_1\psi_2$	$\overline{\psi}_1\gamma^y\tau_2\psi_2\overline{\psi}_2\gamma^y\gamma_5\tau_1\psi_2$	$-i$
$\overline{\psi}_1\gamma^y\gamma_5\tau_1\psi_1\overline{\psi}_1\gamma^y\tau_2\psi_2$	$\overline{\psi}_1\gamma^y\gamma_5\tau_1\psi_2\overline{\psi}_2\gamma^y\tau_2\psi_2$	$+i$
$\overline{\psi}_1\gamma^y\gamma_5\tau_2\psi_1\overline{\psi}_1\gamma^y\tau_1\psi_2$	$\overline{\psi}_1\gamma^y\gamma_5\tau_2\psi_2\overline{\psi}_2\gamma^y\tau_1\psi_2$	$-i$
$\overline{\psi}_1\gamma^z\tau_1\psi_1\overline{\psi}_1\gamma^z\gamma_5\tau_2\psi_2$	$\overline{\psi}_1\gamma^z\tau_1\psi_2\overline{\psi}_2\gamma^z\gamma_5\tau_2\psi_2$	$+i$
$\overline{\psi}_1\gamma^z\tau_2\psi_1\overline{\psi}_1\gamma^z\gamma_5\tau_1\psi_2$	$\overline{\psi}_1\gamma^z\tau_2\psi_2\overline{\psi}_2\gamma^z\gamma_5\tau_1\psi_2$	$-i$
$\overline{\psi}_1\gamma^z\gamma_5\tau_1\psi_1\overline{\psi}_1\gamma^z\tau_2\psi_2$	$\overline{\psi}_1\gamma^z\gamma_5\tau_1\psi_2\overline{\psi}_2\gamma^z\tau_2\psi_2$	$+i$
$\overline{\psi}_1\gamma^z\gamma_5\tau_2\psi_1\overline{\psi}_1\gamma^z\tau_1\psi_2$	$\overline{\psi}_1\gamma^z\gamma_5\tau_2\psi_2\overline{\psi}_2\gamma^z\tau_1\psi_2$	$-i$

Table B.2 : Operators for O_2

$O_2^{(1)}$	$O_2^{(2)}$	Phase
$\overline{\psi}_1\gamma^t\psi_1\overline{\psi}_1\gamma^t\gamma_5\tau_3\psi_2$	$\overline{\psi}_1\gamma^t\psi_2\overline{\psi}_2\gamma^t\gamma_5\tau_3\psi_2$	$+1$
$\overline{\psi}_1\gamma^t\tau_3\psi_1\overline{\psi}_1\gamma^t\gamma_5\psi_2$	$\overline{\psi}_1\gamma^t\tau_3\psi_2\overline{\psi}_2\gamma^t\gamma_5\psi_2$	-1
$\overline{\psi}_1\gamma^t\gamma_5\psi_1\overline{\psi}_1\gamma^t\tau_3\psi_2$	$\overline{\psi}_1\gamma^t\gamma_5\psi_2\overline{\psi}_2\gamma^t\tau_3\psi_2$	$+1$
$\overline{\psi}_1\gamma^t\gamma_5\tau_3\psi_1\overline{\psi}_1\gamma^t\psi_2$	$\overline{\psi}_1\gamma^t\gamma_5\tau_3\psi_2\overline{\psi}_2\gamma^t\psi_2$	-1
$\overline{\psi}_1\gamma^x\psi_1\overline{\psi}_1\gamma^x\gamma_5\tau_3\psi_2$	$\overline{\psi}_1\gamma^x\psi_2\overline{\psi}_2\gamma^x\gamma_5\tau_3\psi_2$	$+1$
$\overline{\psi}_1\gamma^x\tau_3\psi_1\overline{\psi}_1\gamma^x\gamma_5\psi_2$	$\overline{\psi}_1\gamma^x\tau_3\psi_2\overline{\psi}_2\gamma^x\gamma_5\psi_2$	-1
$\overline{\psi}_1\gamma^x\gamma_5\psi_1\overline{\psi}_1\gamma^x\tau_3\psi_2$	$\overline{\psi}_1\gamma^x\gamma_5\psi_2\overline{\psi}_2\gamma^x\tau_3\psi_2$	$+1$
$\overline{\psi}_1\gamma^x\gamma_5\tau_3\psi_1\overline{\psi}_1\gamma^x\psi_2$	$\overline{\psi}_1\gamma^x\gamma_5\tau_3\psi_2\overline{\psi}_2\gamma^x\psi_2$	-1
$\overline{\psi}_1\gamma^y\psi_1\overline{\psi}_1\gamma^y\gamma_5\tau_3\psi_2$	$\overline{\psi}_1\gamma^y\psi_2\overline{\psi}_2\gamma^y\gamma_5\tau_3\psi_2$	$+1$
$\overline{\psi}_1\gamma^y\tau_3\psi_1\overline{\psi}_1\gamma^y\gamma_5\psi_2$	$\overline{\psi}_1\gamma^y\tau_3\psi_2\overline{\psi}_2\gamma^y\gamma_5\psi_2$	-1
$\overline{\psi}_1\gamma^y\gamma_5\psi_1\overline{\psi}_1\gamma^y\tau_3\psi_2$	$\overline{\psi}_1\gamma^y\gamma_5\psi_2\overline{\psi}_2\gamma^y\tau_3\psi_2$	$+1$
$\overline{\psi}_1\gamma^y\gamma_5\tau_3\psi_1\overline{\psi}_1\gamma^y\psi_2$	$\overline{\psi}_1\gamma^y\gamma_5\tau_3\psi_2\overline{\psi}_2\gamma^y\psi_2$	-1
$\overline{\psi}_1\gamma^z\psi_1\overline{\psi}_1\gamma^z\gamma_5\tau_3\psi_2$	$\overline{\psi}_1\gamma^z\psi_2\overline{\psi}_2\gamma^z\gamma_5\tau_3\psi_2$	$+1$
$\overline{\psi}_1\gamma^z\tau_3\psi_1\overline{\psi}_1\gamma^z\gamma_5\psi_2$	$\overline{\psi}_1\gamma^z\tau_3\psi_2\overline{\psi}_2\gamma^z\gamma_5\psi_2$	-1
$\overline{\psi}_1\gamma^z\gamma_5\psi_1\overline{\psi}_1\gamma^z\tau_3\psi_2$	$\overline{\psi}_1\gamma^z\gamma_5\psi_2\overline{\psi}_2\gamma^z\tau_3\psi_2$	$+1$
$\overline{\psi}_1\gamma^z\gamma_5\tau_3\psi_1\overline{\psi}_1\gamma^z\psi_2$	$\overline{\psi}_1\gamma^z\gamma_5\tau_3\psi_2\overline{\psi}_2\gamma^z\psi_2$	-1

Appendix C : The Group Theory

C.1. SU(3) Clebsch–Gordon Coefficients.

We summarize those Clebsch–Gordon coefficients that are needed to execute a Strong Coupling calculation to fourth order. The form of these coefficients is given, for the representation equation, by:

$$N \otimes 3 = M_1 \oplus M_2 \cdots \oplus M_p \tag{C.1}$$

$$\phi_{M_i}{}^{a_1 \cdots a_m}{}_{b_1 \cdots b_n} = C_{M_i N}{}^{a_1 \cdots a_m}{}_{b_1 \cdots b_n}{}^{m_1 \cdots m_p}{}_{n_1 \cdots n_q} [\, \phi_N{}^{n_1 \cdots n_q}{}_{m_1 \cdots m_p} \phi_3{}^{\omega} \,]$$

Product	Components	Clebsch–Gordon Coefficient
$3 \otimes 3$	6	$S^{a_1 a_2}{}_{mn}$
	$\overline{3}$	$\frac{1}{\sqrt{2}} \varepsilon_{amn}$
$3 \otimes \overline{3}$	8	$P_8{}^{a_1}{}_{a_2}{}^{n}{}_{m}$
	1	$\frac{1}{\sqrt{3}} \delta^{n}{}_{m}$
$6 \otimes 3$	10	$S^{a_1 a_2 a_3}{}_{m_1 m_2 n}$
	8	$\left(\frac{2}{3}\right)^{1/2} S^{a_1 \lambda}{}_{m_1 m_2} \varepsilon_{\lambda a_2 n}$
$6 \otimes \overline{3}$	15	$P_{15}{}^{a_1 a_2}{}_{a_3 m_1 m_2}{}^{n}$
	3	$\frac{1}{\sqrt{2}} S^{a_1 n}{}_{m_1 m_2}$

Product	Component	Clebsch–Gordon Coefficient
$8 \otimes 3$	15	$P_{15}{}^{a_1 a_2}{}_{a_3 n m_1}{}^{m_2}$
	$\overline{6}$	$\frac{1}{\sqrt{2}} S^{m_1 \lambda}{}_{a_1 a_2} \varepsilon_{\lambda m_2 n}$
	3	$\left(\frac{3}{8}\right)^{1/2} P_8{}^{a_1}{}_n{}^{m_2}{}_{m_1}$
$10 \otimes 3$	15_1	$S^{a_1 a_2 a_3 a_4}{}_{m_1 m_2 m_3 n}$
	15_2	$\left(\frac{3}{4}\right)^{1/2} S^{a_1 a_2 \lambda}{}_{m_1 m_2 m_3} \varepsilon_{\lambda n a_3}$
$10 \otimes \overline{3}$	24	$P_{24}{}^{a_1 a_2 a_3}{}_{a_4 m_1 m_2 m_3}{}^{n}$
	6	$\left(\frac{3}{5}\right)^{1/2} S^{a_1 a_2 n}{}_{m_1 m_2 m_3}$
$15_2 \otimes 3$	24	$P_{24}{}^{a_1 a_2 a_3}{}_{a_4 n m_1 m_2}{}^{m_3}$
	$\overline{15}_2$	$\left(\frac{2}{3}\right)^{1/2} P_{15}{}^{m_3 \lambda_1}{}_{\lambda_2 a_1 a_2}{}^{a_3} \varepsilon_{\lambda_1 \lambda_3 n} S^{\lambda_2 \lambda_3}{}_{m_1 m_2}$
	6	$\left(\frac{2}{5}\right)^{1/2} P_{15}{}^{a_1 a_2}{}_{n m_1 m_2}{}^{m_3}$
$15_2 \otimes \overline{3}$	27	$P_{27}{}^{a_1 a_2}{}_{a_3 a_4 m_1 m_2}{}^{m_3 n}$
	10	$\frac{1}{\sqrt{2}} P_{15}{}^{a_1 a_2}{}_{a_3 m_1 \lambda_1}{}^{\lambda_2} \varepsilon^{\lambda_1 \lambda_3 n} S^{m_2 m_3}{}_{\lambda_2 \lambda_3}$
	8	$\left(\frac{8}{15}\right)^{1/2} P_{15}{}^{m_1 m_2}{}_{m_3 n a_1}{}^{a_2}$

The Clebsch–Gordon coefficients that we need for $\overline{N} \otimes 3$ or $\overline{N} \otimes \overline{3}$ can be immediately obtained from those above simply by interchanging up and down indices. Hence, because the 8 and 27 representations are self conjugate, $8 \otimes \overline{3}$ and $27 \otimes \overline{3}$ can be likewise obtained. Also notice that there are two types of 15 representation. The 15_1 is fully symmetric on its four indices, the 15_2 has a mixed symmetry. The various projection operators used above are defined, with $N = 3$ obviously, as follows

$$P_8{}^{a_1}{}_{a_2}{}^{m_1}{}_{m2} = \delta^{a_1}{}_{m_2}\delta_{a_2}{}^{m_1} - \frac{1}{N}\delta^{a_1}{}_{a_2}\delta^{m_1}{}_{m_2} \tag{C.2a}$$

$$P_{15}{}^{a_1a_2}{}_{a_3m_1m_2}{}^{m_3} = S^{a_1a_2}{}_{m_1m_2}\delta_{a_3}{}^{m_3} - \frac{2}{(N+2)}S^{a_1a_2}{}_{a_3\lambda}S^{\lambda m_3}{}_{m_1m_2} \tag{C.2b}$$

$$P_{24}{}^{a_1a_2a_3}{}_{a_4m_1m_2m_3}{}^{m_4} = S^{a_1a_2a_3}{}_{m_1m_2m_3}\delta_{a_4}{}^{m_4} \tag{C.2c}$$

$$- \frac{1}{(N+3)}S^{a_1a_2a_3}{}_{a_4\lambda_1\lambda_2}S^{\lambda_1\lambda_2m_4}{}_{m_1m_2m_3}$$

$$P_{27}{}^{a_1a_2}{}_{a_3a_4m_1m_2}{}^{m_3m_4} = S^{a_1a_2}{}_{m_1m_2}S^{m_3m_3}{}_{a_3a_4} \tag{C.2d}$$

$$+ \frac{2}{(N+1)(N+2)}S^{a_1a_2}{}_{a_3a_4}S^{m_3m_4}{}_{m_1m_2}$$

$$- \frac{4}{(N+2)}S^{a_1a_2}{}_{\lambda_1\lambda'_2}S^{\lambda_1\lambda_2}{}_{a_3a_4}S^{\lambda'_1\lambda'_2}{}_{m_1m_2}S^{m_3m_4}{}_{\lambda_2\lambda'_2}$$

C.2. SU(3) Quadratic Casimir Invariants

Representation	Quadratic Casimir
1	0
3	4/3
6	10/3
8	3
10	6
15_1	16/3
15_2	28/3
24	25/3
27	8

C.3. SU(2) Clebsch–Gordan Coefficients

For SU(2) the Clebsch–Gordon coefficients can be written as two simple formulae. The Casimir operator for a representation N is $\frac{1}{4}N(N+1)$.

Product	Component	CG Coefficient
$N \otimes 2$	$N+1$	$S^{a_1 \cdots a_{N+1}}{}_{m_1 \cdots m_N n}$
	$N-1$	$\left[\frac{N-1}{N}\right]^{1/2} S^{a_1 \cdots a_{N-1}\lambda}{}_{m_1 \cdots m_N} \varepsilon_{\lambda n}$

Appendix D : CP Violation

This calculation was done as an afterthought to the main body of this work. We will just review the important formulae, and then present the results.

D.1. The CP Violating Hamiltonian

CP Violation cannot exist within the context of the standard model until we have six quarks. From the results that we obtained in Chap.7.; in particular, the relative unimportance of the c –quark loops, it is obvious that the addition of an additional generation of quarks, the t and b quarks, would not alter the results or conclusions significantly. Hence, for the CP conserving amplitudes we will use the results obtained for the four quark model.

The CP violating piece of the Hamiltonian is given by [1]:

$$\frac{G_F}{\sqrt{2}} \sin\theta_1 \sin\theta_2 \sin\theta_3 \cos\theta_2 \, e^{i\delta} [\, \bar{d}_a \gamma^\mu (1+\gamma_5) c^a \bar{c}_b \gamma_\mu (1+\gamma_5) s^b$$

$$- \bar{d}_a \gamma^\mu (1+\gamma_5) t^a \bar{t}_b \gamma^\mu (1+\gamma_5) s^b] \qquad \text{(D.1)}$$

The values of the KM angles θ_1, θ_2, θ_3, and the phase δ will not concern us because they will cancel out in the final result. We also ignore any corrections that might come from perturbative QCD renormalizations of the derived $O_\pm$ operators.

We now form the ratios [19]:

$$\eta_{+-} = \frac{\langle \pi^+\pi^- | H_W | K_L \rangle}{\langle \pi^+\pi^- | H_W | K_S \rangle} \qquad \text{(D.2a)}$$

$$\eta_{00} = \frac{\langle \pi^0\pi^0 | H_W | K_L \rangle}{\langle \pi^0\pi^0 | H_W | K_S \rangle} \qquad \text{(D.2b)}$$

The phases η_{+-} and η_{00} are now written in terms of the phases ε and ε', viz:

$$\eta_{+-} \approx \varepsilon + \varepsilon' \tag{D.3a}$$

$$\eta_{00} \approx \varepsilon - 2\varepsilon' \tag{D.3b}$$

The ratio ε'/ε is what we will calculate. The current experimental bound is given by [5]:

$$\left| \frac{\varepsilon'}{\varepsilon} \right| < \frac{1}{50} \tag{D.4}$$

D.2. Results

The calculation that we carry out simply reused the raw results that were computed earlier. We take the t quark mass to be forty times that of the c quark. A graph of the results is given in Fig.8. The important point to note is that the ratio changes sign, passing through zero between $0.10 < A_1 < 0.12$. This feature of the result has been commented upon in Chap.7.

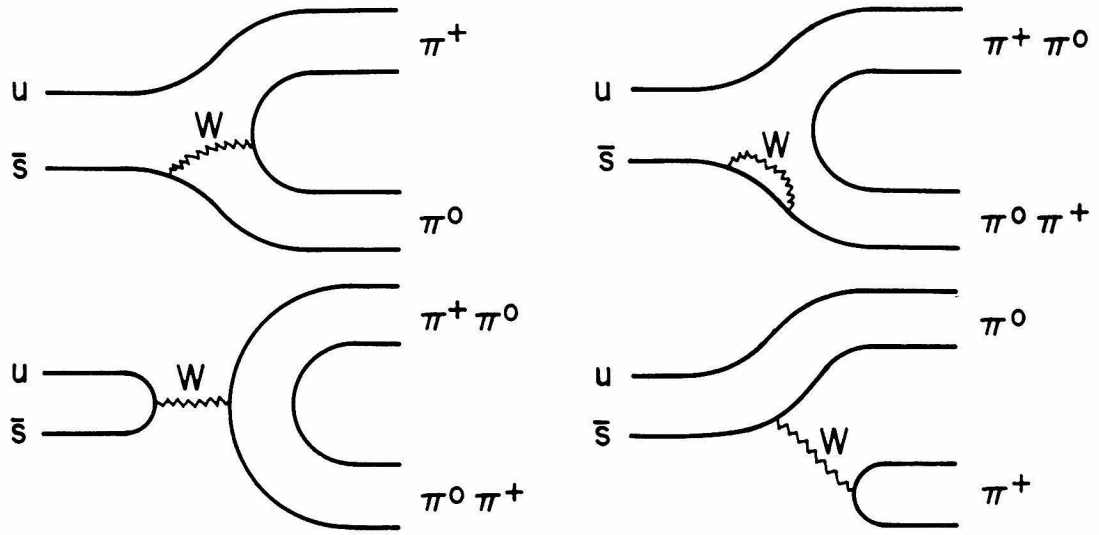

(1a) Feynman Diagrams : K^+ Decays

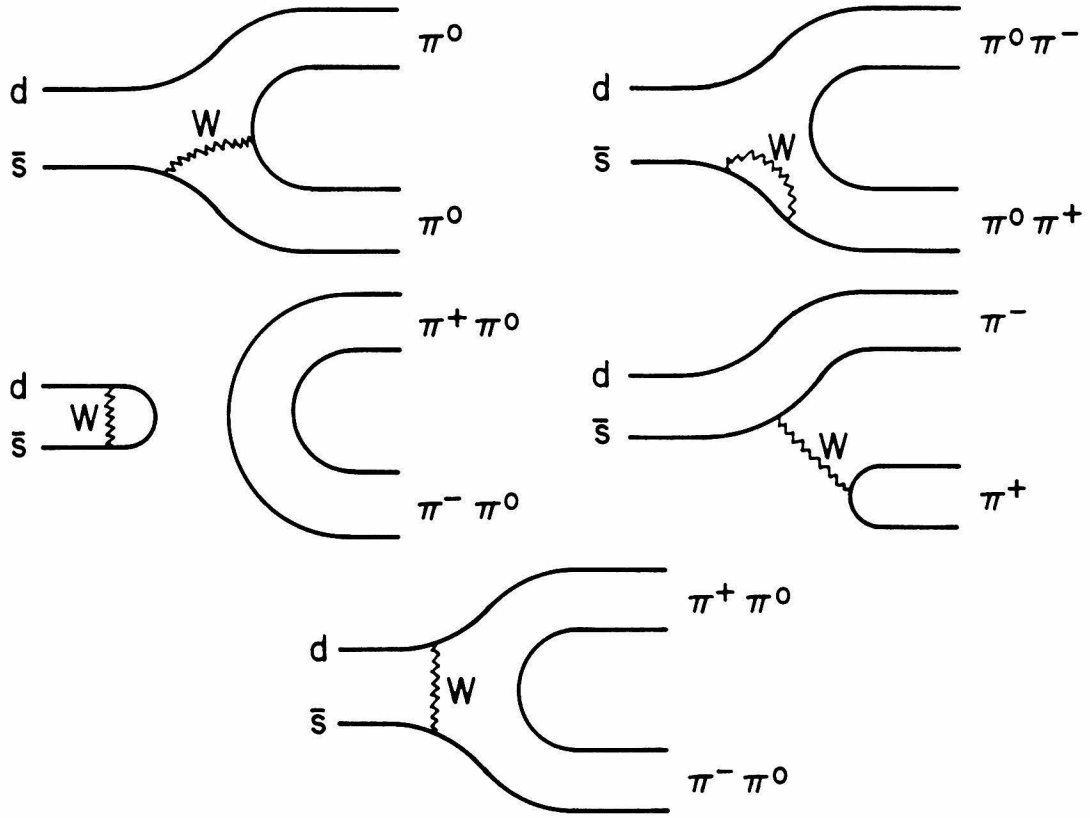

(1b) Feynman Diagrams : K^0 Decays

Figure 1

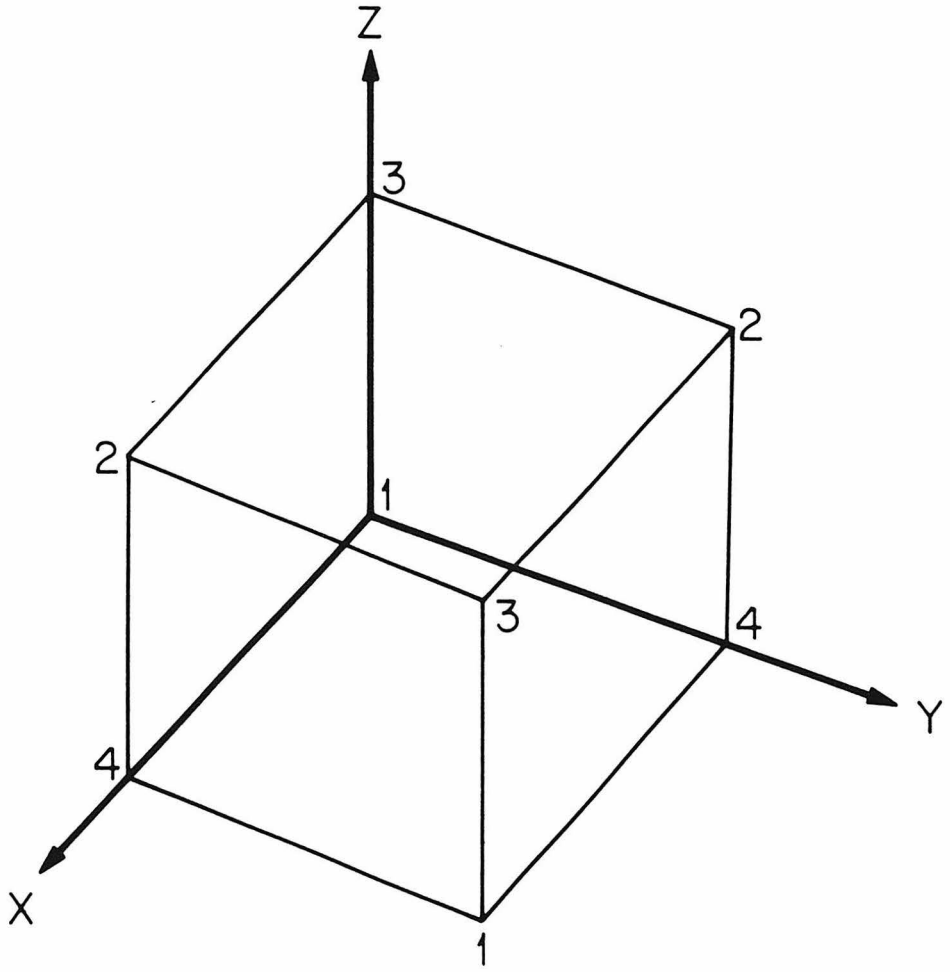

The Kogut-Susskind Fermion Sublattics

Figure 2

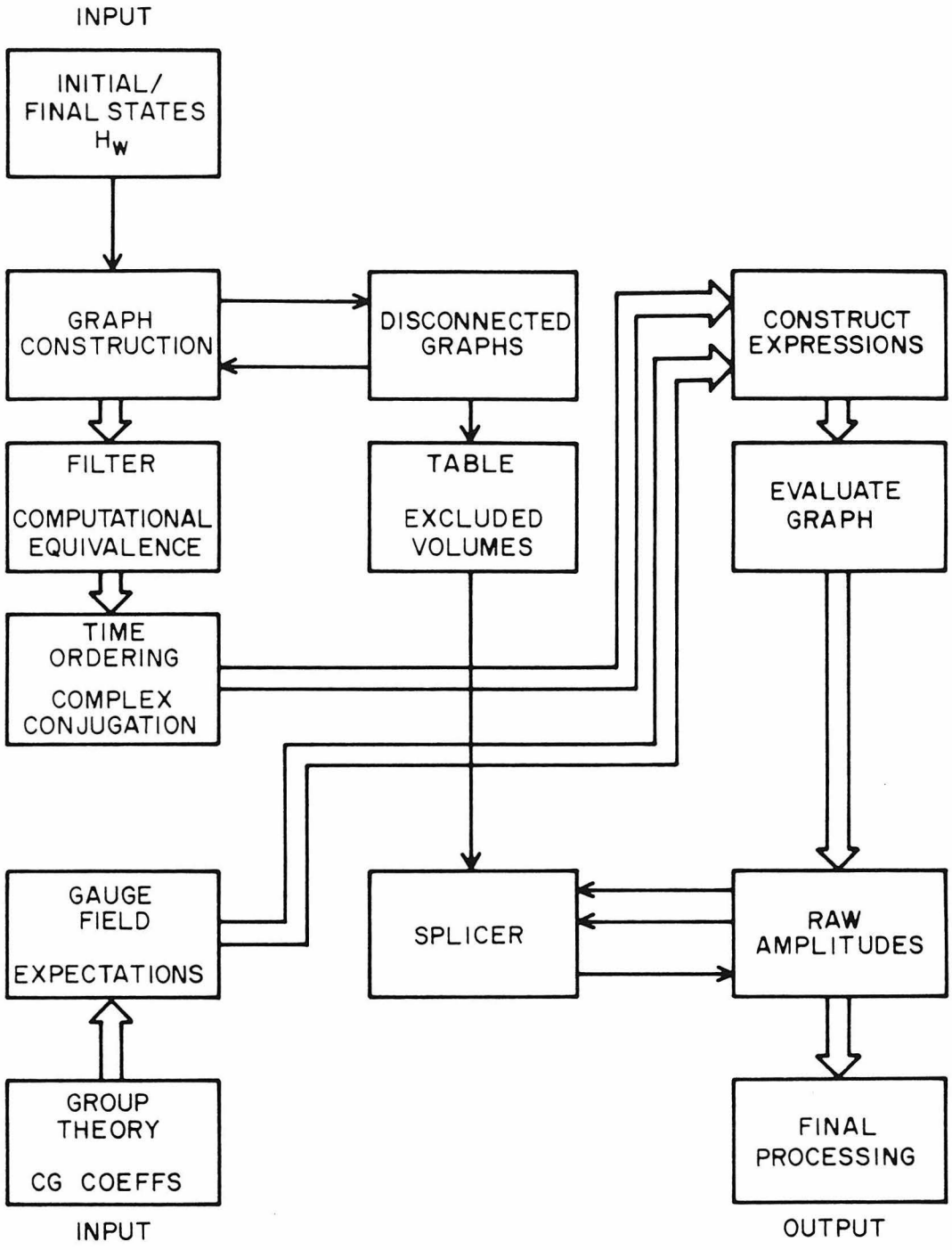

Strong Coupling and Computer Algebra

Figure 3

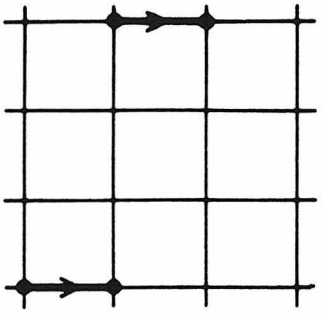

$$E = \frac{8}{3} + 136A_1$$

(4a) Separated

$$E = \frac{8}{3} + 128A_1$$

(4b) Side by side

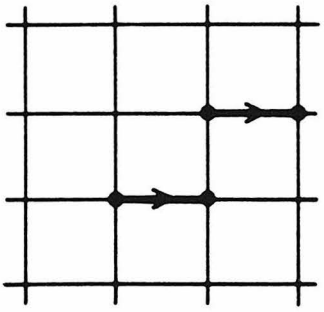

$$E = \frac{8}{3} + 84A_1$$

(4c) Head to tail

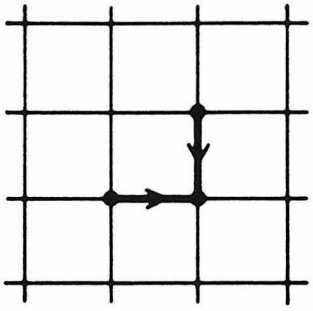

$$E = \frac{4}{3} + 130A_1$$

(4d) Head to head

Components of the Two Pion Wavefunction

Figure 4

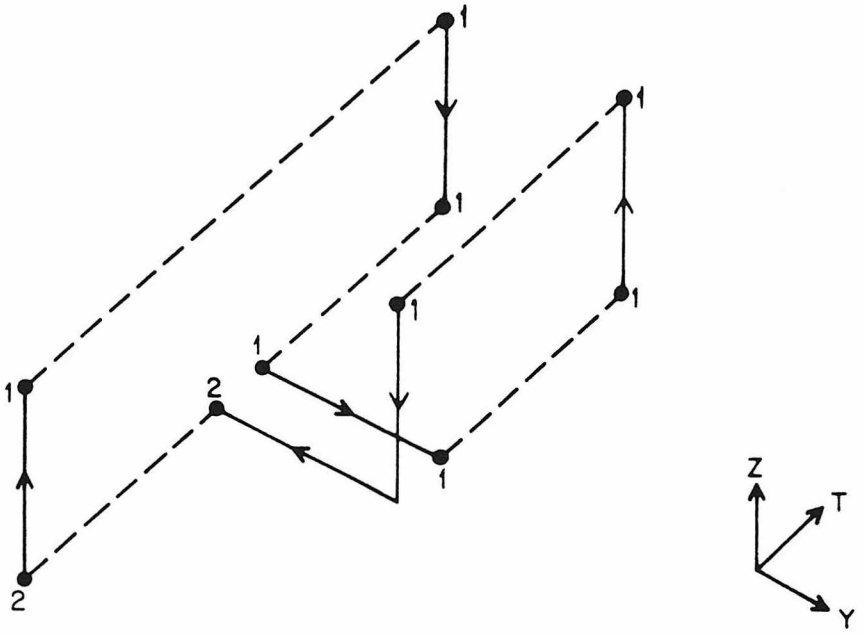

(5a) Zeroth-Order Graph

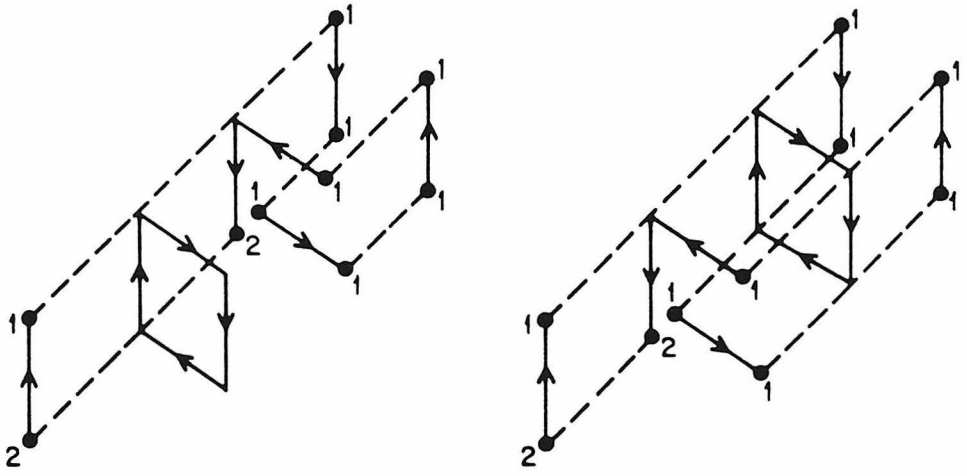

(5b) First-Order Graphs

Figure 5

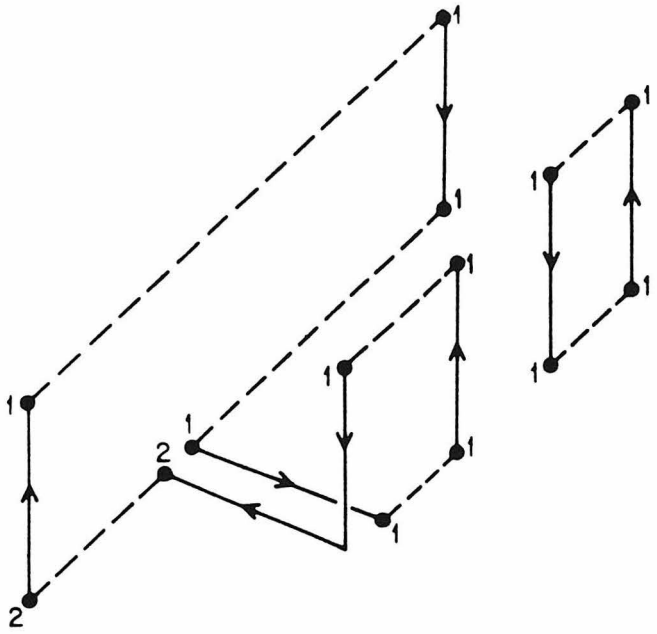

(6a) "Penguin" or "Eye" Graphs; u Loop

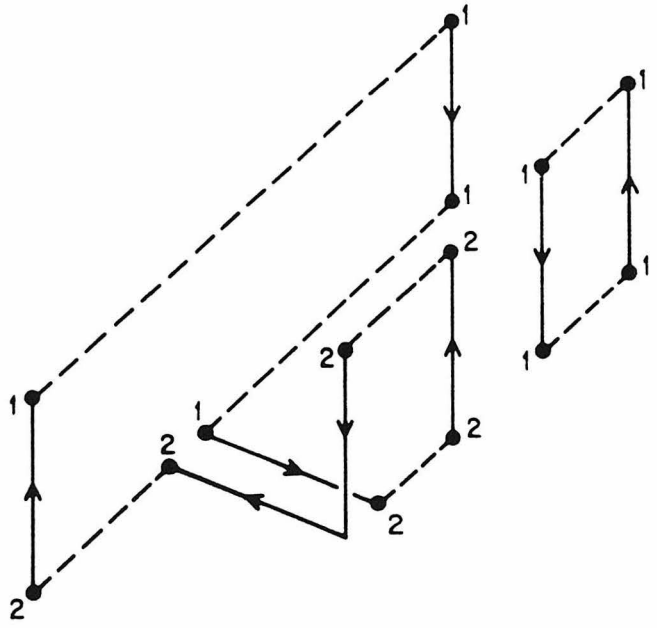

(6b) "Penguin" or "Eye" Graphs; c Loop

Figure 6

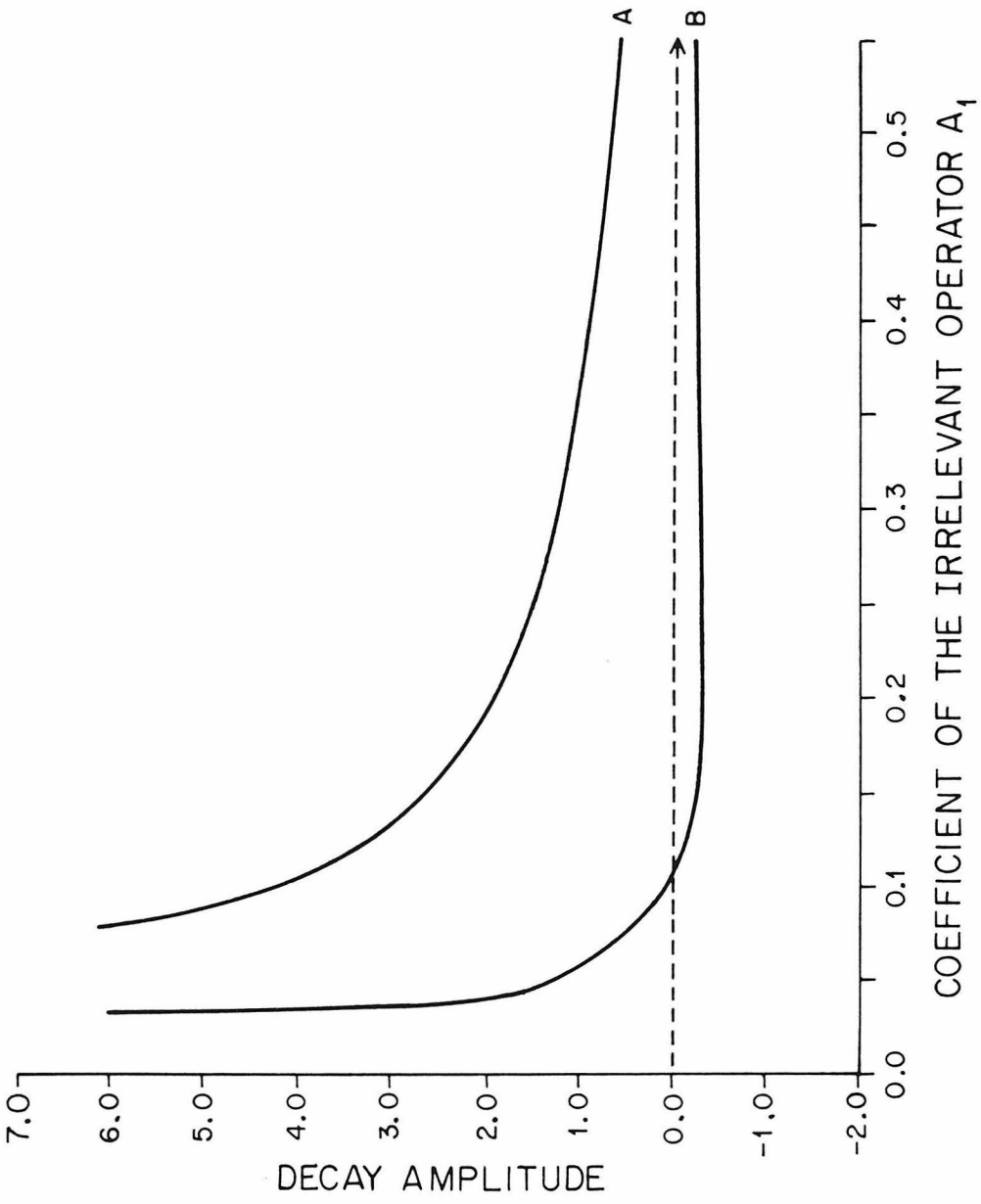

Matrix Elements $\langle 0 | H_W | K \rangle$ (A) and $\langle 2 | H_W | K \rangle$ (B)

Figure 7

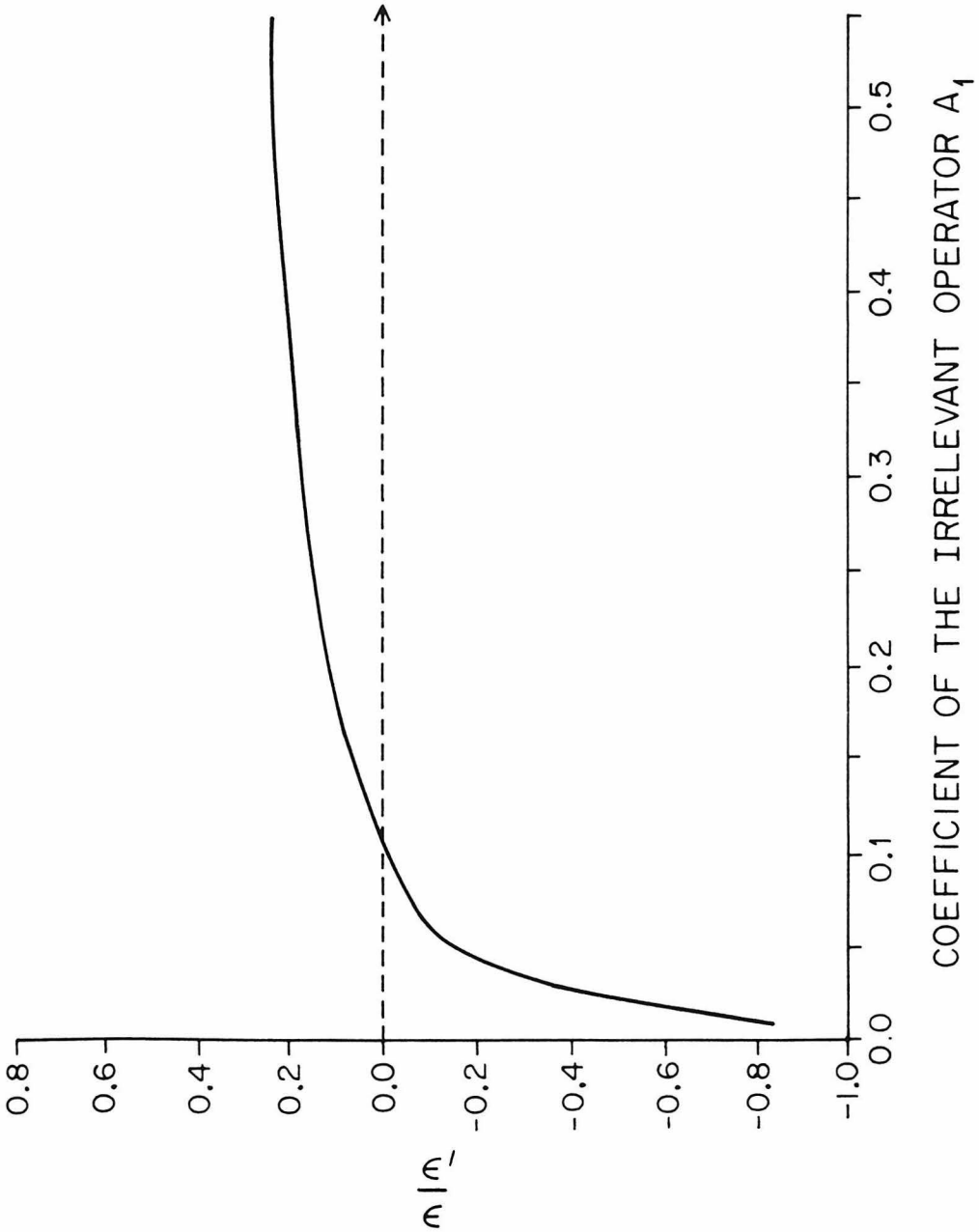

The Ratio $\frac{\varepsilon'}{\varepsilon}$

Figure 8